3q26. Proc Natl Acad Sci U S A. 1992;89:3937-3941.

47. Nucifora G, Begy CR, Kobayashi H, et al. Consistent intergenic splicing and production of multiple transcripts between AML1 at 21q22 and unrelated genes at 3q26 in (3;21)(q26;q22) translocations. Proc Natl Acad Sci U S A. 1994;91:4004-4008.
48. Du Y, Carling T, Fang W, Piao Z, Sheu JC, Huang S. Hypermethylation in human cancers of the RIZ1 tumor suppressor gene, a member of a histone/protein methyltransferase superfamily. Cancer Res. 2001;61:8094-8099.
49. Chadwick RB, Jiang GL, Bennington GA, et al. Candidate tumor suppressor RIZ is frequently involved in colorectal carcinogenesis. Proc Natl Acad Sci U S A. 2000;97:2662-2667.
50. He L, Yu JX, Liu L, et al. RIZ1, but not the alternative RIZ2 product of the same gene, is underexpressed in breast cancer, and forced RIZ1 expression causes G2-M cell cycle arrest and/or apoptosis. Cancer Res. 1998;58:4238-4244.
51. Steele-Perkins G, Fang W, Yang XH, et al. Tumor formation and inactivation of RIZ1, an Rb-binding member of a nuclear protein-methyltransferase superfamily. Genes Dev. 2001;15:2250-2262.
52. Fears S, Mathieu C, Zeleznik-Le N, Huang S, Rowley JD, Nucifora G. Intergenic splicing of MDS1 and EVI1 occurs in normal tissues as well as in myeloid leukemia and produces a new member of the PR domain family. Proc Natl Acad Sci U S A. 1996;93:1642-1647.
53. Rea S, Eisenhaber F, O'Carroll D, et al. Regulation of chromatin structure by site-specific histone H3 methyltransferases. Nature. 2000;406:593-599.
54. Nislow C, Ray E, Pillus L. SET1, a yeast member of the trithorax family, functions in transcriptional silencing and diverse cellular processes. Mol Biol Cell. 1997;8:2421-2436.
55. Nakamura T, Mori T, Tada S, et al. ALL-1 is a histone methyltransferase that assembles a supercomplex of proteins involved in transcriptional regulation. Mol Cell. 2002;10:1119-1128.
56. Huang S, Shao G, Liu L. The PR domain of the Rb-binding zinc finger protein RIZ1 is a protein binding interface and is related to the SET domain functioning in chromatin-mediated gene expression. J Biol Chem. 1998;273:15933-15939.
57. Kurokawa M, Mitani K, Irie K, et al. The oncoprotein Evi-1 represses TGF-beta signalling by inhibiting Smad3. Nature. 1998;394:92-96.
58. Mori N, Morishita M, Tsukazaki T, et al. Human T-cell leukemia virus type I oncoprotein Tax represses Smad-dependent transforming growth factor beta signaling through interaction with CREB-binding protein/p300. Blood. 2001;97:2137-2144.
59. Arnulf B, Villemain A, Nicot C, et al. Human T-cell lymphotropic virus oncoprotein Tax represses TGF-beta 1 signaling in human T cells via c-Jun activation: a potential mechanism of HTLV-I leukemogenesis. Blood. 2002;100:4129-4138.
60. Lee DK, Kim BC, Brady JN, Jeang KT, Kim SJ. Human T-cell lymphotropic virus type 1 tax inhibits transforming growth factor-beta signaling by blocking the association of Smad proteins with Smad-binding element. J Biol Chem. 2002;277:33766-33775.
61. Tamiya S, Matsuoka M, Etoh K, et al. Two types of defective human T-lymphotropic virus type I provirus in adult T-cell leukemia. Blood. 1996;88:3065-3073.
62. Furukawa Y, Kubota R, Tara M, Izumo S, Osame M. Existence of escape mutant in HTLV-I tax during the development of adult T-cell leukemia. Blood. 2001;97:987-993.
63. Takeda S, Maeda M, Morikawa S, et al. Genetic and epigenetic inactivation of tax gene in adult T-cell leukemia cells. Int J Cancer. In press.
64. Bertolesi GE, Shi C, Elbaum L, et al. The Ca(2+) channel antagonists mibefradil and pimozide inhibit cell growth via different cytotoxic mechanisms. Mol Pharmacol. 2002;62:210-219.

Int. J. Cancer: **110**, 621–625 (2004)

Publication of the International Union Against Cancer

LETTER TO THE EDITOR

Role of HTLV-1 Proviral DNA Load and Clonality in the Development of Adult T-Cell Leukemia/Lymphoma in Asymptomatic Carriers

Akihiko OKAYAMA[1]*, Sherri STUVER[2,3], Masao MATSUOKA[4], Junzo ISHIZAKI[1], Gen-ichi TANAKA[1], Yoko KUBUKI[1], Nancy MUELLER[3], Chung-cheng HSIEH[5], Nobuyoshi TACHIBANA[6] and Hirohito TSUBOUCHI[1]

[1]*Department of Internal Medicine II, Miyazaki Medical College, Miyazaki, Japan*
[2]*Department of Epidemiology, Boston University School of Public Health, Boston, MA, USA*
[3]*Department of Epidemiology, Harvard School of Public Health, Boston, MA, USA*
[4]*Laboratory of Virus Immunology, Institute for Virus Research, Kyoto University, Kyoto, Japan*
[5]*Division of Biostatistics and Epidemiology, University of Massachusetts Medical School Cancer Center, Boston, MA, USA*
[6]*Department of Nursing Science, Miyazaki Prefectural Nursing College, Miyazaki, Japan*

Dear Sir,

Human T-lymphotropic virus type 1 (HTLV-1) is the causative agent for adult T-cell leukemia/lymphoma (ATL).[1–3] Only a small proportion of HTLV-1 carriers eventually develop ATL after a long latency.[4] However, the critical events in the leukemogenic process remain unclear. In general, viral load is an important factor affecting the outcome of virus-associated disease. The HTLV-1 proviral DNA load in the peripheral blood mononuclear cells (PBMCs) of carriers exhibits a wide range of values.[5] Enhanced expression of HTLV-1 Tax, which transactivates transcription of viral mRNA and of host genes that control cell proliferation, induces amplification of infected cells (*i.e.,* the number of proviral copies).[6] One of the host genes encodes the IL-2 receptor (IL-2R), which is overexpressed on the surface of ATL cells.[7] We have observed that subjects with detectable *tax/rex* mRNA have a higher number of IL-2Rα-positive T cells.[8] We also have found a positive association between HTLV-1 proviral load and the level of soluble IL-2R in asymptomatic carriers,[5] as well as the number of morphologically abnormal lymphocytes on a peripheral blood smear among carriers.[9,10] In addition, the HTLV-1 proviral load within a carrier is stable over many years.[5] It has been postulated that clonal proliferation of HTLV-1-infected cells likely is responsible for maintaining the proviral load level in a carrier.[11,12] HTLV-1 Tax may contribute to the clonal proliferation of HTLV-1-infected cells by promoting their abnormal growth.[6] Tax also exerts dysregulation of the cell cycle by binding to its inhibitors and inhibiting some tumor-suppressor proteins.[6]

The accumulated data support the hypothesis that increased HTLV-1 proviral load and clonal expansion of HTLV-1-infected cells are key to the process of leukemogenesis in HTLV-1 carriers. However, proviral DNA levels and clonality of HTLV-1-infected cells have not been directly evaluated as predictors of the development of ATL in asymptomatic carriers. Given an ATL incidence rate as low as 1 case per 1,000 person-years among HTLV-1 carriers, such a study would require extensive follow-up of a relatively large number of HTLV-1 carriers.

The Miyazaki Cohort Study is a population-based prospective study of the natural history of HTLV-1, which was established in 1984.[13] During follow-up of the cohort through December 2000, 6 ATL cases were identified through an annual census or reports from next-of-kin.[14] Four of the 6 cases had available prediagnostic samples of PBMCs and were included in the present analysis (Table I). Diagnosis was confirmed by medical records for 3 of the 4 cases (cases 1, 3, 4). Lymph node biopsy for case 4 and the PBMCs at ATL diagnosis for cases 1 and 4 were available for analysis. Any symptoms suggestive of smoldering- or chronic-type ATL, such as skin lesions or lymphadenopathy, were not observed at the annual health examinations prior to the diagnosis of malignancy in the cases studied. Routine blood tests performed at the annual health examinations also did not reveal any abnormal findings suggestive of subclinical ATL. Therefore, it is unlikely that these cases had smoldering- or chronic-type ATL before the onset of acute- or lymphoma-type ATL. For comparison of HTLV-1 proviral load, age- and sex-matched HTLV-1$^+$ controls were randomly selected from asymptomatic carriers within the cohort. Informed consent was obtained from all study participants, and the study protocol was approved by the Human Subjects Committees of Miyazaki Medical College and Harvard School of Public Health.

HTLV-1 proviral DNA in PBMCs was quantitated using the AmpliSensor assay (AcuGen HTLV-1 Quantitation Test; Biotronics, Lowell, MA).[5,15] Prediagnostic HTLV-1 proviral loads of the 4 ATL cases are shown in Table I. Two cases were male (cases 1, 2), and 2 were female (cases 3, 4). Median age at onset of ATL was 73.5 years (range 64–83). Median HTLV-1 proviral load (copies per 100,000 PBMCs) at the earliest prediagnostic PBMC sample (collected 3–8 years prior to ATL onset) was 4,930 (range 830–10,560). Median proviral

Grant sponsor: National Institutes of Health; Grant number: CA38450; Grant sponsor: Ministry of Education, Science, Sports and Culture (Japan).

*Correspondence to: Department of Internal Medicine II, Miyazaki Medical College, 5200 Kihara, Kiyotake, Miyazaki 8891601, Japan. Fax: +81-985-85-5194. E-mail: okayama@post1.miyazaki-med.ac.jp

Received 16 September 2003; Revised 17 December 2003; Accepted 7 January 2004

DOI 10.1002/ijc.20144
Published online 15 March 2004 in Wiley InterScience (www.interscience.wiley.com).

TABLE I – HTLV-1 PROVIRAL DNA LOADS IN 4 CARRIERS WHO EVENTUALLY DEVELOPED ATL

	Case 1	Case 2	Case 3	Case 4
Year before onset				
8				6,690[1]
7			830	
6				
5	3,170		1,910	2,200
4			1,480	
3		10,560		
2			2,110	18,150
1			2,840	
ATL type at diagnosis	Acute	Not available	Lymphoma	Lymphoma
Age[2] (years), sex	83, male	64, male	76, female	70, female

[1]Copies per 100,000 PBMCs.–[2]Age at death.

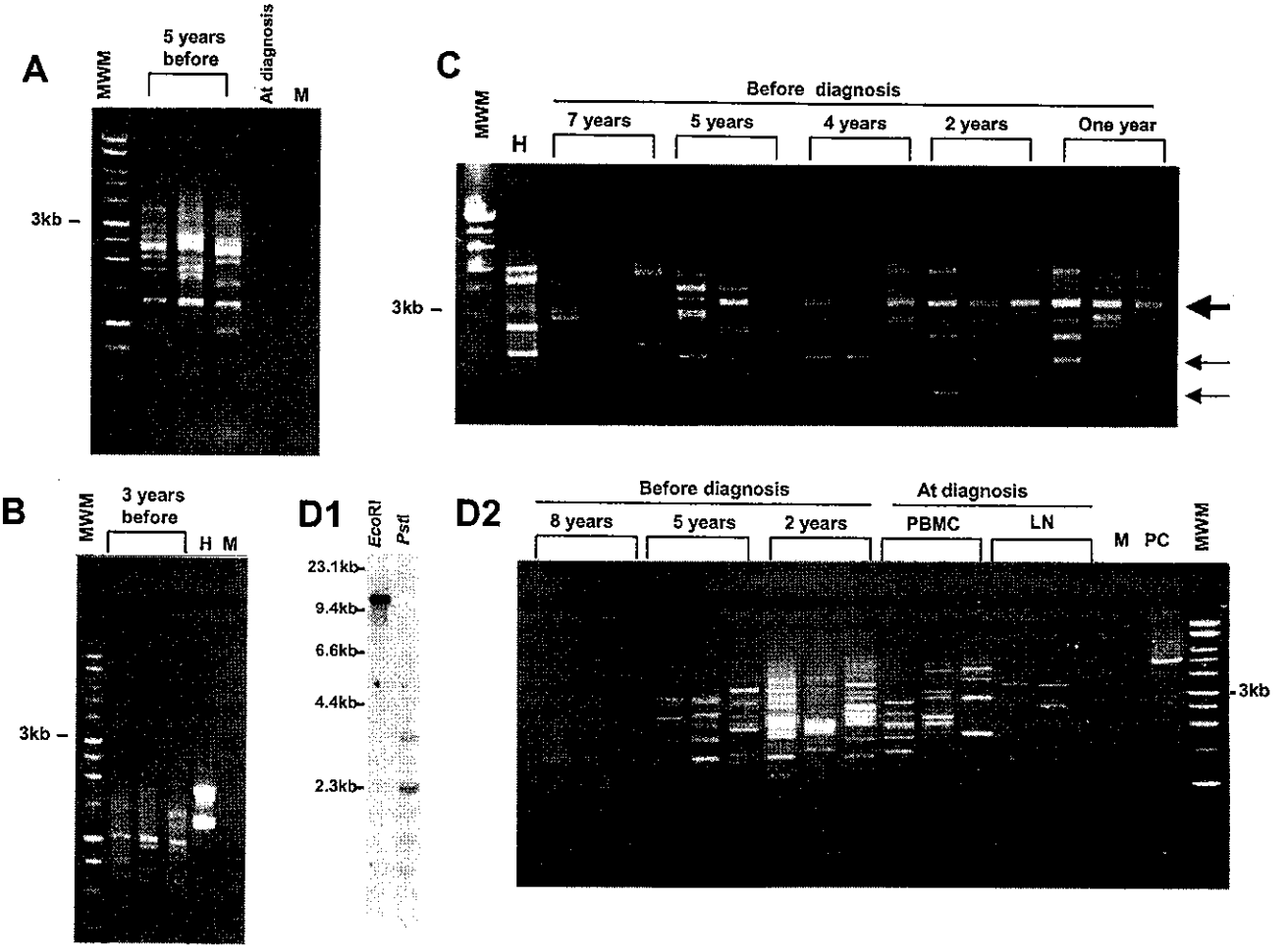

FIGURE 1 – Inverse-long PCR analysis of HTLV-1-infected cells in 4 cases before and at diagnosis of ATL. *(a)* Case 1. Triplicate analysis of PBMCs in the sample obtained 5 years before the onset of ATL and single analysis of ATL cells at diagnosis. *(b)* Case 2. Triplicate analysis of PBMCs in the sample obtained 3 years before the onset of ATL. *(c)* Case 3. Triplicate analysis of PBMCs in samples obtained 1–7 years before the onset of ATL. Arrows indicate major clones. *(d1)* Case 4. Southern blot analysis of lymph node biopsy specimen at diagnosis. EcoRI, EcoRI digestion; PstI, PstI digestion. *(d2)* Case 4. Triplicate inverse-long PCR analysis of PBMCs in samples obtained 2–8 years before the onset of ATL and from PBMC and lymph node (LN) samples obtained at diagnosis. MWM, m.w. marker (1 kb ladder); H, HUT102 cells as HTLV-1-positive control; M, Molt4 cells as HTLV-1-negative control; PC, leukemic cells obtained from an ATL patient, who was not a member of the study cohort, as a control.

load of the 37 age- and sex-matched HTLV-1$^+$ control subjects was 820 (10–9,790), which was significantly lower than the earliest prediagnostic proviral load of cases (Wilcoxon rank sum test, $p = 0.03$). In conditional logistic regression analysis, which accounted for the matched design (LogXact 4.1; Cytel, Cambridge, MA), there was a significant association between higher viral load and case status; the odds ratio of being an ATL case associated with each 1,000 copies (per 100,000 PBMCs) increase in viral load was 1.42 (95% exact confidence interval 1.04–2.10, $p = 0.03$).

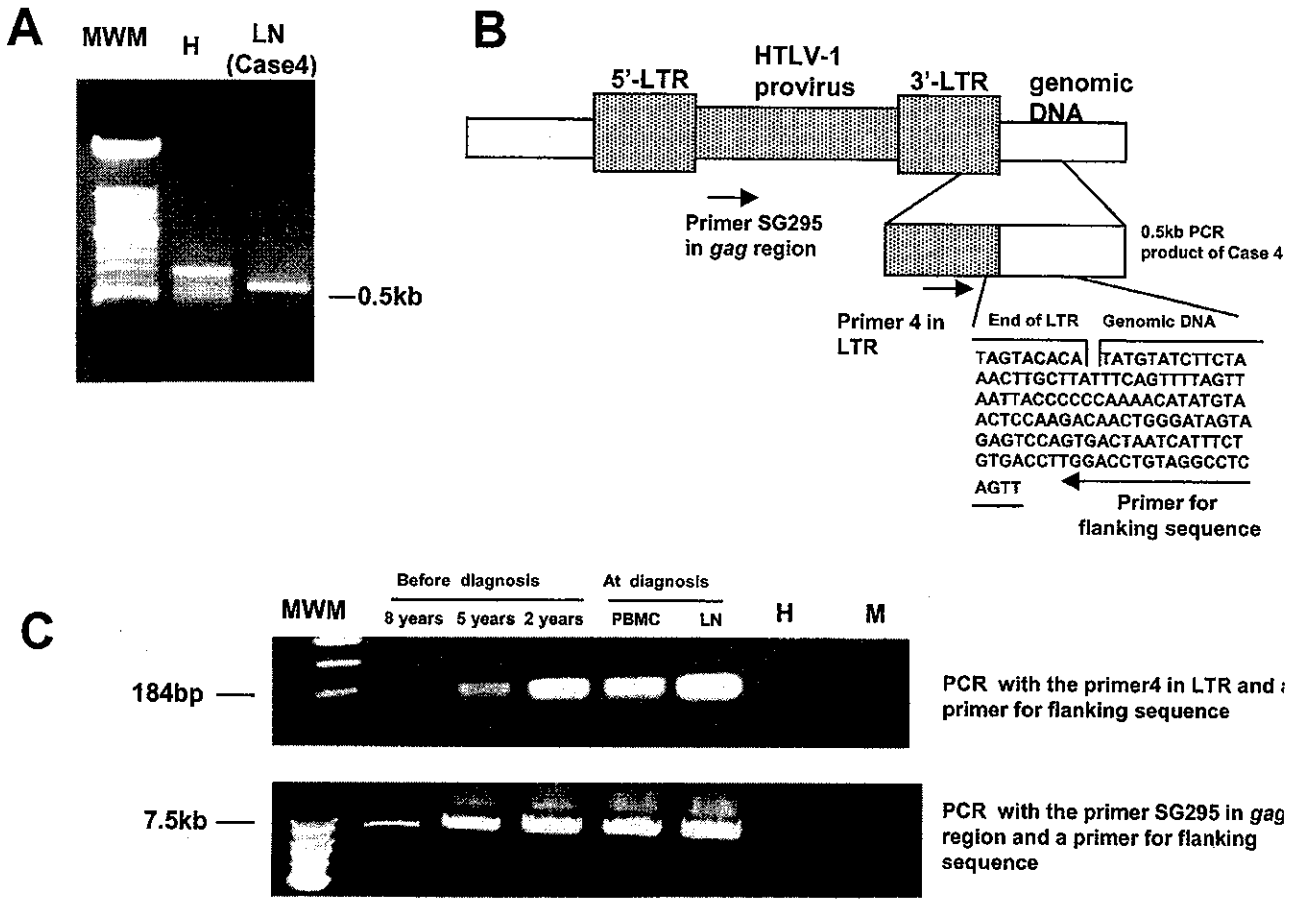

FIGURE 2 – Detection of the preleukemic clone in PBMC samples obtained from case 4 before diagnosis of ATL. *(a)* Inverse PCR analysis of lymph node (LN) specimen obtained at ATL diagnosis. *(b)* Schema showing subcloned and sequenced DNA of the inverse PCR amplicon derived from case 4 and the locations of primers used for leukemic clone-specific PCR. *(c)* Leukemic clone-specific PCR analysis using primer 4 of the LTR (upper panel) and primer SG295 (lower panel) before and at diagnosis of ATL. MWM, m.w. marker; H, HUT102 cells as HTLV-1-positive control; M, Molt4 cells as HTLV-1-negative control.

Although the number of cases analyzed was small, the difference in proviral load between cases and controls was striking and statistically significant. Our prospective analysis, thus, demonstrates an association between higher proviral DNA load and the subsequent development of ATL. HTLV-1 proviral DNA levels were stable over several years in asymptomatic carriers.[5] In cases 3 and 4, who had PBMC samples from more than 5 years, proviral levels were increased in samples obtained closest to the time of ATL diagnosis (1 and 2 years before onset, respectively). These increased proviral loads may reflect the clonal expansion of certain HTLV-1-infected cells.

Because the primers of the *pol* region were used for the quantitative assay of proviral DNA load, HTLV-1-infected cells with *pol*-defective provirus could not be detected by the current method. It is possible that the HTLV-1-infected cells with such defective virus were seen more commonly in carriers who developed ATL rather than in the control group because the defective provirus is sometimes found in patients with ATL.[16] As a result, the difference in proviral DNA load between cases and controls might have been larger if we had used a more conserved region, such as *tax*, for the primers.

We also examined whether the preleukemic HTLV-1-infected clone can be found prior to diagnosis in the peripheral blood of carriers who go on to develop ATL. To amplify the genomic DNA adjacent to the integration sites of the HTLV-1 provirus, inverse long-PCR was used.[12] All 4 cases had clonal bands of various sizes and intensities, indicating oligoclonal or polyclonal expansion of HTLV-1-harboring cells prior to diagnosis (Fig. 1). For case 1, a single band indicating the leukemic clone was detected in the peripheral blood by inverse long-PCR at diagnosis (Fig. 1*a*). Case 3, a carrier who developed lymphoma-type ATL, had several bands that were consistently strong over several years (arrows in Fig. 1*c*). These bands appear to represent major clones, consisting of large numbers of HTLV-1-infected cells with the same proviral integration site. One of the bands increased in intensity in the samples obtained close to the onset of ATL (large arrow in Fig. 1*c*). However, it was not possible to determine whether this clone was the preleukemic one because a sample from the time of ATL diagnosis for this carrier was not available.

For case 4, monoclonal integration of the HTLV-1 provirus in the leukemic cells from the lymph node was demonstrated by Southern blot assay at diagnosis (Fig. 1*d1*). However, the

leukemic clone was undetectable by inverse long-PCR, and only some faint bands were seen in the lymph node sample obtained at the time of ATL diagnosis (Fig. 1*d2*). This observation is not surprising since leukemic clones are reported to be detectable only in about half of patients by inverse long-PCR due to the lack of adequate sites for restriction enzymes or to sequence deficiencies of the HTLV-1 provirus in leukemic cells.[12]

To identify the preleukemic clone in the peripheral blood of case 4 prior to diagnosis, the nucleotide sequence of the 3′ flanking region of the integrated provirus in the ATL cells first was determined using the inverse PCR method (Fig. 2*a,b*).[17] We then synthesized a primer (5′-AACTGAGGCCTACAG-GTCCA-3′) that would specifically amplify the junction site of the 3′ long terminal repeat (LTR). Using this leukemic clone-specific primer, the HTLV-1-infected cell clone with the same integration site of the provirus as the leukemic cells was detectable 2, 5 and 8 years before the onset of ATL, with 2 different primers for the HTLV-1 LTR (primer 4 used in inverse PCR) and *gag* sequences (primer SG295) (Fig. 2*c*).[18] The intensity of this clone was increased at 2 years prior to ATL diagnosis compared to the intensity at 5 and 8 years before diagnosis (Fig. 2*c*).

In addition, case 4 was diagnosed as lymphoma-type, and leukemic cells were rarely observed in the peripheral blood smear at diagnosis. However, clone-specific PCR was strongly positive not only in the lymph node but also in the peripheral blood of case 4. This observation suggests that preleukemic cells without morphologic abnormality, which belonged to the original clone, existed in the peripheral blood even at diagnosis of ATL. At some point during the 8 years before ATL onset in this case, a subclone could have acquired additional malignant potential, presumably due to genetic and epigenetic abnormalities. Indeed, the presence of multiple clones of ATL cells based on the methylation patterns of the *CDKN2A* gene, despite having the same HTLV-1 integration site, has been reported.[19] It also has been reported that multiple clones with simple chromosomal abnormalities already exist in HTLV-1 carriers and that selected clones with more complex chromosomal abnormalities can be found in progressed chronic ATL, based on the clonal culture method.[20] Therefore, HTLV-1 carriers are hypothesized to vary with respect to the genetic and epigenetic abnormalities of their HTLV-1-infected cells. The risk of developing ATL might be related to these differences among HTLV-1 carriers.

In case 1, a clone with the same integration site of the provirus in the leukemic cells was not detectable in the PBMC sample obtained 5 years before the onset of ATL (data not shown). This finding could be due to insufficient sensitivity of the PCR assay to detect that particular clone.

In conclusion, the present prospective study provides evidence that a higher proviral DNA load strongly predicts the development of ATL in asymptomatic HTLV-I carriers. Moreover, the preleukemic clone can be observed in peripheral blood as many as 8 years before onset of the malignancy. This particular finding supports the belief that persistent clonal expansion is important in leukemogenesis. Thus, measuring the proviral DNA load and determining the clonality of HTLV-1-infected cells may provide important information for identifying carriers at increased risk of ATL. Further studies to characterize the level of genetic and epigenetic abnormalities accumulated in HTLV-1-infected cells will be necessary for the development of prophylactic therapies.

Yours sincerely,

Akihiko OKAYAMA, Sherri STUVER, Masao MATSUOKA, Junzo ISHIZAKI, Gen-ichi TANAKA, Yoko KUBUKI, Nancy MUELLER, Chung-cheng HSIEH, Nobuyoshi TACHIBANA and Hirohito TSUBOUCHI

REFERENCES

1. Poiesz BJ, Ruscetti FW, Gazdar AF, Bunn PA, Minna JD, Gallo RC. Detection and isolation of type-C retrovirus particles from fresh and cultured lymphocytes of a patient with cutaneous T-cell lymphoma. Proc Natl Acad Sci USA 1980;77:7415–9.
2. Hinuma Y, Nagata K, Hanaoka M, Nakai M, Matsumoto T, Kinoshita KI, Shirakawa S, Miyoshi I. Adult T-cell leukemia: antigen in an ATL cell line and detection of antibodies to the antigen in human sera. Proc Natl Acad Sci USA 1981;78:6476–80.
3. Yoshida M, Miyoshi I, Hinuma Y. Isolation and characterization of retrovirus from cell lines of human adult T-cell leukemia and its implication in the disease. Proc Natl Acad Sci USA 1982;79:2031–5.
4. Tajima K, Kamura S, Ito S, Ito M, Nagatomo M, Kinoshita K, Ikeda S. Epidemiological features of HTLV-I carriers and incidence of ATL in an ATL-endemic island: a report of the community-based cooperative study in Tsushima, Japan. Int J Cancer 1987;40:741–6.
5. Etoh K, Yamaguchi K, Tokudome S, Watanabe T, Okayama A, Stuver S, Mueller N, Takatsuki K, Matsuoka M. Rapid quantification of HTLV-I provirus load: detection of monoclonal proliferation of HTLV-1 infected cells among blood donors. Int J Cancer 1999;81: 859–64.
6. Yoshida, M. Multiple viral strategies of HTLV-1 for dysregulation of cell growth control. Annu Rev Immunol 2001;19:475–96.
7. Uchiyama T, Hori T, Tsudo M, Wano Y, Umadome H, Tamori S, Yodoi J, Maeda M, Sawami H, Uchino H. Interleukin-2 receptor (Tac antigen) expressed on adult T cell leukemia cells. J Clin Invest 1985;76:446–53.
8. Okayama A, Tachibana N, Ishihara S, Nagatomo Y, Murai K, Okamoto M, Shima T, Sagawa K, Tsubouchi H, Stuver S, Mueller N. Increased expression of interleukin-2 receptor α on peripheral blood mononuclear cells in HTLV-I tax/rex mRNA-positive asymptomatic carriers. J Acquir Immune Defic Syndr Hum Retrovirol 1997;15: 70–5.
9. Tachibana N, Okayama A, Ishihara S, Shioiri S, Murai K, Tsuda K, Goya N, Matsuo Y, Essex M, Stuver S, Mueller N. High HTLV-I proviral DNA level associated with abnormal lymphocytes in peripheral blood from asymptomatic carriers. Int J Cancer 1992;51:593–5.
10. Hisada M, Okayama A, Tachibana N, Stuver SO, Spiegelman DL, Tsubouchi H, Mueller NE. Predictors of level of circulating abnormal lymphocytes among human T-lymphotropic virus type I carriers in Japan. Int J Cancer 1998;77:182–92.
11. Cavrois M, Leclercq I, Gout O, Gessain A, Wain-Hobson S, Wattel E. Persistent oligoclonal expansion of human T-cell leukemia virus type 1–infected circulating cells in patients with tropical spastic paraparesis/HTLV-1 associated myelopathy. Oncogene 1998;17:77–82.
12. Etoh K, Tamiya S, Yamaguchi K, Okayama A, Tsubouchi H, Ideta T, Mueller N, Takatsuki K, Matsuoka M. Persistent clonal proliferation of human T-lymphotropic virus type I-infected cells in vivo. Cancer Res 1997;57:4862–7.
13. Mueller N, Tachibana N, Stuver S, Okayama, A, Ishizaki J, Shishime E, Murai K, Shioiri S, Tsuda K. Epidemiologic perspectives of HTLV-I. In: Blattner WA, ed. Human retrovirology. New York: Raven, 1990. 281–93.
14. Hisada M, Okayama A, Shioiri S, Spiegelman DL, Stuver SO, Mueller NE. Risk factors for adult T-cell leukemia among carriers of human T-lymphotropic virus type I. Blood 1998;92:3557–61.
15. Okayama A, Stuver S, Iga M, Okamoto M, Mueller N, Matsuoka M, Yamaguchi K, Tachibana N, Tsubouchi H. Sequential change of viral markers in seroconverters with community-acquired infection of human T-lymphotropic virus type 1. J Infect Dis 2001;183:1031–7.
16. Korber B, Okayama A, Donnerlly R, Tachibana N, Essex M. Polymerase chain reaction analysis of defective human T-cell leukemia

virus type I proviral genomes in leukemic cells of patients with adult T-cell leukemia. J Virol 1991;65:5471–6.
17. Takemoto S, Matsuoka M, Yamaguchi K, Takatsuki K. A novel diagnostic method of adult T-cell leukemia: monoclonal integration of human T-cell lymphotropic virus type I provirus DNA detected by inverse polymerase chain reaction. Blood 1994;84:3080–5.
18. Ehrlich GD, Greenberg S, Abbott MA. Detection of human T-cell lymphoma/leukemia viruses. In: Innis MA, Gelfand DH, Sninsky JJ, White TJ, eds. PCR protocols. San Diego: Academic, 1990. 325–36.
19. Nosaka K, Maeda M, Tamiya S, Sakai T, Mitsuya H, Matsuoka M. Increasing methylation of the *CDKN2A* gene is associated with the progression of adult T-cell leukemia. Cancer Res 2000;60: 1043–8.
20. Fujimoto T, Hata T, Itoyama T, Nakamura H, Tsukasaki K, Yamada Y, Ikeda S, Sadamori N, Tomonaga M. High rate of chromosomal abnormalities in HTLV-1-infected T-cell colonies derived from prodromal phase of adult T-cell leukemia: a study of IL-2-stimulated colony formation in methylcellulose. Cancer Genet Cytogenet 1999; 109:1–13.

Int. J. Cancer: **109**, 559–567 (2004)

Publication of the International Union Against Cancer

GENETIC AND EPIGENETIC INACTIVATION OF *TAX* GENE IN ADULT T-CELL LEUKEMIA CELLS

Satoshi TAKEDA[1], Michiyuki MAEDA[2], Shigeru MORIKAWA[3], Yuko TANIGUCHI[1], Jun-ichirou YASUNAGA[4], Kisato NOSAKA[1], Yuetsu TANAKA[5], and Masao MATSUOKA[1]*

[1]*Institute for Virus Research, Kyoto University, Kyoto, Japan*
[2]*Institute for Frontier Medical Science, Kyoto University, Kyoto, Japan*
[3]*Department of Pathology, First Unit, Shimane Medical University, Shimane, Japan*
[4]*Department of Internal Medicine II, Kumamoto University School of Medicine, Kumamoto, Japan*
[5]*Department of Infectious Disease and Immunology, Okinawa-Asia Research Center of Medical Science, University of the Ryukyu, Okinawa, Japan*

To clarify the status of *tax* gene, we analyzed human T-cell leukemia virus type-I (HTLV-I) associated cell lines and fresh adult T-cell leukemia (ATL) cells. We compared 2 types of HTLV-I associated cell lines: one was derived from leukemic cells (leukemic cell line) and the other from nonleukemic cells (nonleukemic cell line). Although all nonleukemic cell lines expressed Tax, it could not be detected in 3 of 5 leukemic cell lines, in which nonsense mutation or deletion (60 bp) of *tax* genes, and DNA methylation in 5′-LTR were identified as the responsible changes. We found such genetic changes of the *tax* gene in 5 of 47 fresh ATL cases (11%). The *tax* gene transcripts could be detected in 14 of 41 fresh ATL cases (34%) by RT-PCR. In ATL cases with genetic changes that could not produce Tax protein, the *tax* gene was frequently transcribed, suggesting that such cells do not need the transcriptional silencing. Although DNA methylation of 5′-LTR was detected in the fresh ATL cases (19 of 28 cases; 68%), the complete methylation associated with transcriptional silencing was observed only in 4 cases. Since partial methylation could not silence the transcription, and the *tax* gene transcription was not detected in 27 of 41 cases (66%), the epigenetic change(s) other than DNA methylation is considered to play an important role in the silencing.

Key words: *HTLV-I; ATL; tax; DNA methylation; leukemia*

Adult T-cell leukemia (ATL) is a neoplastic disease derived from helper T-lymphocytes and is considered as a distinct clinical entity based on clinical features and geographic distribution of patients.[1,2] Identification of the causative agent, HTLV-I, has allowed detailed analysis of the epidemiological, immunological and clinical characteristics of ATL.[3–6] There are 4 clinical subtypes of ATL: smoldering, chronic, acute and lymphoma-type ATL. The first 2 types exhibit insidious clinical course and after several years progress to acute or lymphoma-type ATL. Acute and lymphoma-type ATL are clinically aggressive forms with a mean survival time of about 1 year in spite of intensive chemotherapy. HTLV-I transmits mainly from mother to child *via* breast milk. The relative risk of development of ATL among carriers has been estimated in Japan to be about 5% after a long latent period of approximately 60 years.[7] It is suggested that the process of leukemogenesis depends on multiple steps and is influenced by various factors such as viral protein.[8]

Tax is an important HTLV-I viral protein and is encoded by the pX region between *env* and 3′-long terminal repeat (LTR).[5] Tax is thought to play a central role in ATL leukemogenesis by its pleiotropic actions such as transactivation of NFκB, CREB and SRF pathways,[9,10] and functional inactivation of p16, p53 and MAD1.[11–13] However, the enigma of Tax-induced leukemogenesis is that the expression of Tax in leukemic cells remains unclear. In some ATL cells, deletion of 5′-LTR,[15] which is a promoter of viral genes, and nonsense mutation of *tax* gene result in the loss of Tax protein.[16] It is noteworthy that these changes are predominantly observed in the aggressive forms of ATL like acute and lymphoma-type ATL.

In the present study, we analyzed the *tax* gene in HTLV-I associated cell lines and fresh ATL cells, and identified the mechanisms that inactivated *tax* gene in Tax nonexpressing cell lines.

MATERIAL AND METHODS

Cells

Eight HTLV-I-associated cell lines were used in the present study: 5 (ED, ATL-43T, ATL-48T, ATL-55T and ATL-2) were derived from a leukemic clone identified *in vivo* by the same integration sites of HTLV-I provirus or recombination of T-cell receptor genes.[17–20] The remaining 3 cell lines (MT-2, Sez627 and ATL-35T) were not derived from leukemic cells. The human embryonic kidney cell line, 293, was studied as a control. To study the effect of demethylation, ATL-43T was cultured in media supplemented with 10 μM 5-aza-2′-deoxycytidine (5-Aza-CdR) (Sigma Chemical Co., St. Louis, MO) for 3 days or 10 μM 5-Aza-CdR and 1 μM trichostatin A (TSA) (Sigma Chemical Co.) for the last 24 hr, and then followed by isolation of RNAs and proteins.

Peripheral blood mononuclear cells (PBMCs) were isolated from patients with ATL. Clinical subtypes of ATL were diagnosed as reported by Shimoyama *et al.*[21] The percentage of CD4-positive cells among lymphocyte population was > 90% in each case examined. The subjects were 47 patients with ATL (30 cases with acute ATL, 4 with lymphoma-type ATL and 13 with chronic ATL). The diagnosis of ATL was confirmed by the monoclonal integration of HTLV-I provirus in the host genome by the Southern blot method.

Abbreviations: 5-Aza-CdR, 5-aza-2′-deoxycytidine; ATL, adult T-cell leukemia; ChIP, Chromatin immunoprecipitation; HTLV-I, human T-cell leukemia virus type I; LTR, long terminal repeat; PBMC, Peripheral blood mononuclear cell; TRE, Tax-responsive element; TSA, trichostatin A

Grant sponsor: Ministry of Education, Science, Sports and Culture of Japan; Grant sponsor: Welfide Medicinal Research Foundation; Grant sponsor: Public Trust Haraguchi Memorial Cancer Research Fund.

Dr. Shigeru Morikawa deceased after the submission.

*Correspondence to: Institute of Virus Research, Kyoto University, 53 *Shogoin* Kawahara-cho, Sakyo-ku, Kyoto, Japan 606-8507, Japan. Fax: +81-75-751-4049. E-mail: mmatsuok@virus.kyoto-u.ac.jp

Received 24 April 2003; Revised 10 September 2003, 17 October 2003; Accepted 24 October 2003

DOI 10.1002/ijc.20007
Published online 9 January 2004 in Wiley InterScience (www.interscience.wiley.com).

cDNA synthesis and direct sequencing

Total RNAs were isolated from the cell lines and fresh ATL cells using Trizol reagent (Life Technologies, Inc., Paisley, UK) and cDNAs were prepared from 1 μg of total RNAs using the RNA LA PCR Kit (Takara, Shiga, Japan) as described by the manufacturer. Oligo dT primers were used to prime first-strand synthesis for the entire reaction. For PCR, 1 μl of the reverse transcriptase reaction mixture was diluted with 50 μl of PCR buffer containing 0.2 mM each of deoxynucleotide triphosphates, 1.5 mM $MgCl_2$, 1.25 unit of Taq DNA polymerase (Takara) and 20 pmol of each primer. Primers used for RT-PCR were as follows: *tax* gene; 5′-CCGGCGCTGCTCTCATCCCGGT-3′ (sense) and 5′-GGCCGAACATAGTCCCCCAGAG-3′ (antisense). PCR was performed in the GeneAmp 2400 (Applied BioSystems, Foster City, CA) for 40 cycles under the following conditions: 2 min at 94°C and 40 cycles of 30 sec at 94°C, 30 sec at 61°C, 2 min at 72°C and finally 2 min at 72°C. Sequencing was performed using Big Dye Terminator (Applied BioSystems) with an ABI 377 autosequencer (Applied BioSystems).

Immunoblot analysis

Total proteins were isolated using RIPA buffer [1% Nonidet P-40, 0.5% sodium deoxycholate, and 0.1% sodium dodecyl sulfate (SDS)]. The 20 μg of protein with protease inhibitors (0.1 mg/ml PMSF, 3% Aprotinin, 1 mM sodium orthovanadate) was separated on SDS-10% polyacrylamide gel electrophoresis and transferred onto nitrocellulose membranes. The membranes were blocked overnight at 4°C with 5% bovine serum albumin, 5% skim milk and 0.01% NaN_3 in PBS containing 0.1% Tween 20. After washing, anti-Tax (Lt-4)[22] or anti-α-tubulin antibody was incubated with the membrane for 1 hr at room temperature, and a horseradish peroxidase conjugate anti-mouse IgG was used during the final 40 min of incubation. Chemiluminescent detection of blotted proteins was performed with an enhanced chemiluminescence kit (Amersham Biosciences Corp., Piscataway, NJ).

Long PCR

Long PCR was performed by a hot start PCR amplification with AmpliWax (Applied BioSystems) as described previously.[15] The lower mixture contained 1×LA PCR buffer II (Mg^{++}-free; Takara), 1.5 mM $MgCl_2$, 0.3 μM of each primer and 0.2 mM deoxynucleotide triphosphates. The upper mixture contained 1×LA PCR buffer II (Mg^{++}-free), 0.5 units of ExTaq (Takara) and 0.2 μg of genomic DNA. PCR cycle conditions were as follows: 25 cycles of 15 sec at 94°C, 30 sec at 68°C and 10 min at 72°C. Sequences of primers used in these experiments were as follows: primer 1; 5′-GTTCCACCCCTTTCCCTTTCATTCACGACTGACTGC-3′; primer 2; 5′-GGCTCTAAGCCCCCGGGGGATATTTGGGGCTCATGG-3′; primer 3; 5′-GGGGTCCCAGGTGATCTGATGCTCTGGACAGGTGGC-3′; primer 4; 5′-GGCGACTGGTGCCCCATCTCTGGGGGACTATGTTCG-3′. To amplify the entire provirus, primers 1 and 2 were used. To determine the deletion of 5′ LTR (defective type 2), the sets of primers 1 and 3 or primers 2 and 4 were used for PCR.

Determination of genomic sequence adjacent to 5′-LTR

To amplify the genomic DNA adjacent to 5′-LTR, we used inverse long PCR as described previously.[23] In brief, the genomic DNAs (1 μg) were digested with *Pst* I and then ligated by T4-DNA ligase. The circularized DNA was used as a substrate for nested PCR. We performed the first PCR (40 cycles) with LA Taq (Takara) as follows: denaturation at 94°C for 30 sec, annealing at 61°C for 30 sec and extension at 72°C for 5 min, followed by a final 10 min extension at 72°C, and the second PCR as follows: denaturation at 94°C for 30 sec, annealing at 57°C for 30 sec and extension at 72°C for 5 min, followed by a final 10 min extension at 72°C. Primers used in this experiment were as follows: the first PCR, 5′-AAGCAAGAAGTCTCCCAAGC-3′ (*gag*: 1261—1280) (sense) and 5′-AGTTAAGCCAGTGATGAGCG-3′ (*gag*: 861–880) (antisense); the second PCR, 5′-CCAGTTTATGCAGACCATCC-3′ (*gag*: 1296–1315) (sense) and 5′-TTCAGACTTCTGTTTCTCGG-3′ (U3: 64–83) (antisense). The numbering of nucleic acids was in reference to ATK-1 according to Seiki *et al.*[5] The sequence of PCR product was determined as described above.

DNA methylation of U3 region determined by sequencing of sodium bisulfite-treated genomic DNAs

DNA methylation was detected by sequencing of PCR products, which were amplified with sodium bisulfite-treated genomic DNAs as described previously.[20] In brief, 1.0 μg DNA samples were denatured by the addition of the same volume of 0.6 M NaOH and then incubated for 15 min at 37°C. Then, 208 μl of 3.6 M sodium bisulfite (pH 5.0) and 12 μl of 10 μM hydroquinone were added to the samples. The samples were covered by mineral oil and then incubated at 55°C for 16 hr. The treated DNAs were purified using Wizard DNA Clean-Up System (Promega, Madison, WI) and then incubated for 10 min in 0.3 N NaOH following the ethanol precipitation. The sodium bisulfite-treated DNAs were amplified by nested PCR with specific primers to the U3 region of HTLV-I LTR, and the genomic sequence of integration site as described above (5′-LTR) or pX region (3′-LTR) as follows: the first PCR, 5′-GGTGTGAGATGGTATTTTATTGTGG-3′ (the genomic sequence adjacent to 5′-LTR of ATL-43T) (sense) or 5′-(C/T)GATGGTA(C/T)GTTTATGATTTT(C/T)GGG-3′(pX) (sense) and 5′-AACTCCTATTATTTTATTAAACC(A/G)TATAC(A/G)-3′(U3) (antisense); the second PCR 5′-GGTGTGAGATGGTATTTTATTGTGG-3′ (the genomic sequence adjacent to 5′-LTR of ATL-43T) (sense) or 5′-(C/T)GATGGTA(C/T)GTTTATGATTTT(C/T)GGG-3′(pX) (sense) and 5′-CC(A/G)TATAC(A/G)TACCATAAAAA-3′ (U3) (antisense). The conditions for PCR were as follows; the first PCR was carried out for 35 cycles (30 sec at 94°C, 30 sec at 47°C (for 5′-LTR) or 49°C (for 3′-LTR), and 30 sec at 72°C) and followed by a final 2 min extension at 72°C, and the second PCR was performed for 40 cycles (30 sec at 94°C, 30 sec at 54°C (for 5′- and 3′-LTR), and 30 sec at 72°C) and followed by a final 2 min extension at 72°C. The final PCR products were subcloned into TOPO XL PCR Cloning kit (Invitrogen, Carlsbad, CA), and the sequences of each clone were determined. DNA methylation of 5′-LTR in the fresh ATL cells was determined using the specific primers to the integration sites of each case.

Methylation specific PCR (MS-PCR)

MS-PCR was performed as described previously by Herman *et al.*[24] Sodium bisulfite treated DNA was first amplified with PCR primers in U3 region of 5′-LTR and *gag* region, and then amplified by primers in R region and *gag* region. Primers were made to anneal to methylated and unmethylated sequences after treatment by sodium bisulfite. Primers were as follows: the first PCR, 5′-TTAAGTCGTTTTTAGGCGTTGAC-3′ (U3; methylated) (sense) or 5′-TTAAGTTGTTTTTAGGTGTTGAT -3′(U3; unmethylated) (sense) and 5′-AAAAAAATTTAACCCATTACC-3′ (*gag*) (antisense); the second PCR 5′- GAGGTCGTTATTTACGTCGGTTGAGTC-3′ (R; methylated) (sense) or 5′- GAGGTTGTTATTTATGTTGGTTGAGTT-3′ (R; unmethylated) (sense) and 5′-AAAAAAATTTAACCCATTACC - 3′ (*gag*) (antisense). The conditions for PCR were as follows; the first PCR was carried out for 35 cycles [30 sec at 95°C, 30 sec at 53°C (for methylated and unmethylated), and 40 sec at 72°C] and followed by a final 2 min extension at 72°C, and the second PCR was performed for 35 cycles [30 sec at 95°C, 30 sec at 52°C (for methylated) or 57°C (for unmethylated) and 30 sec at 72°C] and followed by a final 2 min extension at 72°C.

Quantification of tax *gene transcript*

Transcriptions of *tax* and *GAPDH* (internal control) genes were quantified with real-time PCR as described previously.[25] Probes and primers for *tax* and *GAPDH* genes were designed for quantification. The sequences of primers and probe for *tax* and *GAPDH* genes were as follows; tax primers; 5′-CCGCCGATCCCAAA-

GAA-3′ (sense) and 5′-CTCTGTCCAAACCCTGGGAA-3′ (antisense); *tax* probe; 5′-AAGACCACCAACACCA TGGCCCA-3′; *GAPDH* primers; 5′-ACCAACTGCTTAGCACCCCT-3′ (sense); 5′-GTCTTCTGGGTGGCAGTGAT-3′ (antisense); and *GAPDH* probe; 5′-CTTTGGTATCGTGGAAGGACTCATGACC-3′. The probes were labeled with fluorescent 6-carboxyfluorescein (FAM) (reporter) at the 5′ end and fluorescent 6-carboxy tetramethyl rhodamine (TAMRA) (quencher) at the 3′ end. A part (1/40) of RT-PCR products synthesized from 5 μg total RNA were used for real-time PCR in a 50 μl amplification reaction solution containing 1 × TaqMan buffer A, 3.5 μM $MgCl_2$, 200 μM each of dATP, dCTP, dGTP, 400 μM dUTP, 1.25 unit of AmpliTaq Gold polymerase, 0.5 unit of AmpErase UNG, 300 nM of each primers and 200 nM of the probe. The reaction conditions were 95°C for 10 min (activation of the AmpliTaq Gold polymerase), 40 cycles of 15 sec at 95°C (denaturing) followed by 60 sec at 56°C (for *tax*) or 60°C (for *GAPDH*) (annealing and extension). All experiments were performed and analyzed by the ABI PRISM 7700 Sequence Detection System (Applied BioSystems). To compare the gene expression, we measured the expression of *tax* gene relative to that of *GAPDH* gene.

Chromatin immunoprecipitation assay

Chromatin immunoprecipitation (ChIP) assays were performed as previously described.[26] In brief, ATL cell lines (ATL-43T and ATL-55T) and the fresh ATL cells from an acute ATL patient (5×10^5 cells/antibody) were fixed with formaldehyde and then sonicated to obtain soluble chromatin. The chromatin solutions were immunoprecipitated with 4 μl of anti-acetylated histone H3 antibody, anti-acetylated histone H4 (Upstate Biotechnology, Lake Placid, NY), or normal rabbit IgG overnight at 4°C, and then the immunoprecipitates were collected with 50% protein A and G-Sepharose slurry preabsorbed with 0.1 mg/ml sonicated salmon sperm DNA. Consequent purified DNAs were subjected to PCR reactions using primer sets specific for 5′-LTR. Primers used are as follows: ATL-43T; 5′-GCTACTCAGAGATAACCACTGC-3′ (sense), ATL-55T; 5′-GTCACCACGTACAGCAAGAA-3′ (sense), case 1; 5′-GGGAGCTGAACTGCATTATC-3′ (sense), and U3 region of LTR; 5′-TAAACTTACCTAGACGGCGG-3′ (antisense primer for all PCR reactions). The condition for PCR was as follows; 2 min at 94°C and 35 cycles of 30 sec at 94°C, 30 sec at 62.5°C (ATL-43T and 55T) or 61°C (ATL sample), 45 sec at 72°C, and finally 2 min at 72°C. PCR products were separated on agarose gel and the results were quantified using ATTO densitometry software. Values were calculated as signal intensity of samples normalized by input DNA.

RESULTS

Tax in HTLV-I associated cell lines derived from leukemic and nonleukemic cells

HTLV-I can transform T-lymphocytes *in vitro* similar to the transformation of B-lymphocytes by Epstein-Barr Virus (EBV).[18] When PBMCs from patients with ATL are cultured in the presence of IL-2, most of established cell lines are derived from nonleukemic cells [nonleukemic (NL) cell line].[19] However, a few cell lines were derived from leukemic cells [leukemic (L) cell line]. To clarify the role of Tax in leukemogenesis, we first characterized the expression of Tax in HTLV-I associated cell lines. Tax was expressed in all NL cell lines and 2 L cell lines (ATL-2 and ATL-48T), whereas 3 of the L cell lines (ED, ATL-43T and ATL-55T) did not produce Tax protein (Fig. 1*a*). To clarify the underlying mechanism of the lack of Tax expression in these cell lines, we analyzed the sequences of cDNAs and genomic DNAs of HTLV-I proviruses. HTLV-I proviruses identified in ED contained nonsense mutation (W56*) as shown in Figure 1*b*. On the other hand, RT-PCR detected somewhat larger *tax* gene transcript from ATL-55T than wild-type *tax* transcript as shown in Figure 1*a*. Sequencing of this product revealed that a 60 bp deletion containing the third exon of *tax* gene resulted in aberrant splicing and premature termination in ATL-55T (Fig. 1*c*). However, ATL-43T contained a complete provirus, and the coding sequences for *tax* gene were intact (data not shown), suggesting that mechanism(s) other than mutation or deletion suppressed the transcription of *tax* gene.

DNA methylation in 5′-LTR of ATL-43T

The intact HTLV-I provirus sequence encoding *tax* gene in ATL-43T suggested the role of transcriptional silencing for the lack of Tax protein in this cell line. Therefore, we analyzed DNA methylation of 21 bp repeats [Tax-responsive element (TRE)-1] and TRE-2 within U3 region of LTR.[27–29] To distinguish 5′- and 3′-LTR, we studied each U3 region, which has been shown to be critical for viral transcription, of 5′- and 3′-LTR using sodium bisulfite-treated DNA from ATL-43T. The U3 region of 5′-LTR was amplified with the primer derived from genomic sequence of integration site, which was determined by inverse PCR, and that in U3 region. Genomic sequence adjacent to 5′-LTR of ATL-43T was identified in 7p15.3 (Genbank: AC006377). The U3 region of 3′-LTR was amplified by the primer in pX region and that in the U3 region as described in Material and Methods. Then, the PCR product was subcloned into plasmid DNA, and the sequences of 10 clones from each PCR products were determined (Fig. 2). Only CpG sites in the U3 region of 5′-LTR was heavily methylated whereas there were no methylated CpG sites in the U3 region of 3′-LTR. Indeed, CpG sites were present in CRE site of TRE-1 sites, which has been shown to interact with binding proteins *in vivo*,[30] and most of CpG sites in TRE-1 sites were methylated in ATL-43T. It was noteworthy that the promoter-proximal TRE-1 that was critical for Tax-induced viral transcription was completely methylated in ATL-43T.[30] Since 5′-LTR was the promoter for viral transcription, this result suggested that viral transcription was silenced by the selective DNA methylation of 5′-LTR.

Reactivated expression of Tax protein in ATL-43T

To clarify the role of DNA methylation in the silencing of viral transcription, ATL-43T was treated with a demethylating agent, 5-aza-2′-deoxycytidine (5-Aza-CdR), or 5-Aza-CdR and a histone deacetylase inhibitor, trichostatin A (TSA), which has a synergistic effect with 5-Aza-CdR.[31] To study the transcription of *tax* gene, the transcripts were quantified using real-time PCR as shown in Figure 3*a*. The transcription of *tax* gene was reactivated by 5-Aza-CdR and augmented by addition of TSA in ATL-43T. Furthermore, Tax protein was also produced in ATL-43T cells after treatment with 5-Aza-CdR and increased by addition of TSA (Fig. 3*b*). Treatment only with TSA could not reactivate the *tax* gene transcription (data not shown). These data showed that for reactivation of the *tax* gene transcription, the removal of methylated CpG was indispensable, and deacetylation of histones showed augmented effect.[32,33]

Status of tax *gene in primary ATL cells*

To clarify the significance of *tax* gene in fresh ATL cells, we analyzed the types of provirus, sequences and expression of *tax* gene in ATL cells from 47 ATL cases. Among 47 cases, genetic changes in the *tax* gene, which included nonsense mutation, deletion and insertion, were identified in 5 cases (11%) (Table I). The transcripts of *tax* gene were analyzed by RT-PCR (Fig. 4). In MT-1 cell line, Western blot analysis could not detect Tax protein (data not shown). However, RT-PCR could detect the *tax* gene transcripts. On the other hand, no transcripts were observed in ATL-43T, and HTLV-I carriers by RT-PCR in our study. Since HTLV-I infected, nonleukemic cells might exist in the mononuclear cells from the patients, it is quite difficult to distinguish whether the *tax* gene transcripts were derived from leukemic cells or not. However, the finding that RT-PCR could not detect the *tax* gene transcripts in HTLV-I carrier suggested that it is less likely that detected *tax* gene transcripts were derived from HTLV-I infected, nonleukemic cells. Among ATL cases in which intact

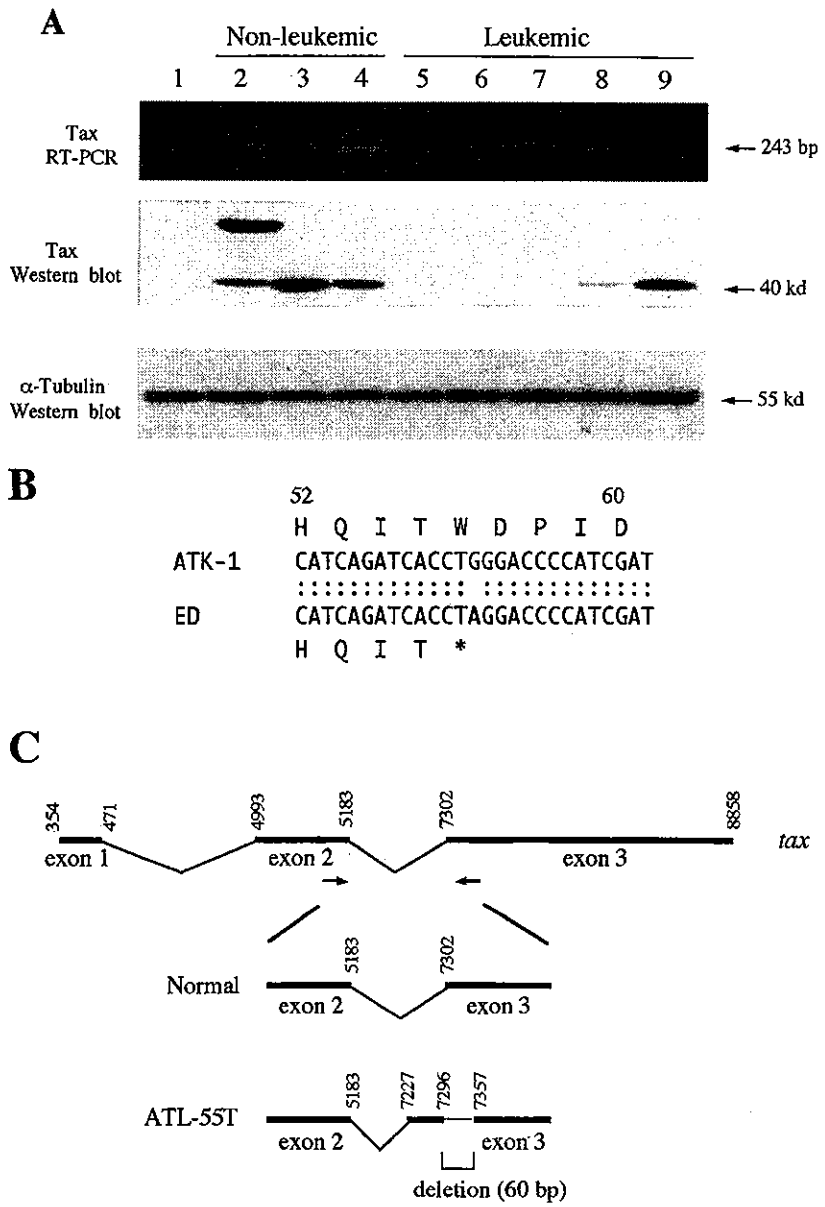

FIGURE 1 – Expression and structure of *tax* genes in HTLV-I associated cell lines. Expressions of *tax* transcripts and Tax proteins were studied by RT-PCR and Western blot analysis (*a*). Lane 1, 293; lane 2, MT-2; lane 3, Sez627; lane 4, ATL-35T; lane 5, ATL-43T; lane 6, ED; lane 7, ATL-55T; lane 8, ATL-48T; lane 9, ATL-2. Structure of *tax* gene in 2 cell lines derived from Tax nonproducing leukemic cells (*b*,*c*). Nonsense mutation was identified (W56*) in ED cell line (*b*), and a deletion (60 bp) containing splicing acceptor site of the third exon of *tax* gene was noted in ATL-55T (*c*). The numbering of peptide, nucleic acids was in reference to ATK-1 according to Seiki *et al.*[5]

mRNAs were available, we found the *tax* gene transcripts in 14 out of 41 cases (34%). Interestingly, the *tax* gene transcripts could be detected in 3 of 4 cases with abortive genetic changes in the *tax* gene (cases 15, 20, 39 and 43), showing that the *tax* gene was transcribed when Tax protein could not be produced. This suggests that such ATL cells, which could not produce intact Tax protein, do not need to silence the viral transcription.

We previously reported that 5′-LTR was preferentially deleted in ATL, which was designated as type 2 defective provirus. Since 5′-LTR is the promoter of viral genes, such provirus is thought to impair the transcription of viral gene. This type of provirus was observed in 14 out of 47 cases (30%). Among 14 ATL cases with type 2 defective provirus, 5 lacked the second exon of *tax* that existed in *env* region, and internal promoter in *pol* region. Among ATL cases with type 2 defective provirus, the *tax* gene transcription was detected in 3 cases, indicating that lack of 5′-LTR is not sufficient for silencing of viral transcription, and in such cases, the internal promoter or trapped cellular promoter drives the transcription. In ATL cells without 5′-LTR and internal promoter, the *tax* gene transcript was not detected.

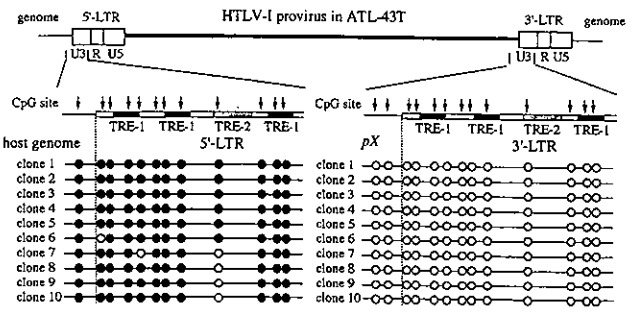

FIGURE 2 – DNA methylation in 5′ and 3′-LTR in HTLV-I provirus of ATL-43T. U3 regions of 5′- and 3′-LTRs were amplified separately with sodium bisulfite-treated genomic DNA, and methylated CpG sites were identified. PCR products were subcloned into plasmid, and 10 clones from each PCR product were sequenced. Closed circles: methylated CpG sites, open circles: unmethylated CpG sites. Tax-responsive element (TRE)-1 and TRE-2 are shown as black and hatched regions, respectively.

DNA methylation of 5′-LTR in primary ATL cells

To study the third mechanism of inactivating Tax production, DNA methylation, we first determined methylated CpGs of 5′-LTR in 4 cases by sodium bisulfite sequencing (cases 1, 2, 3 and 35). As shown in Figure 5, 5′-LTRs were heavily methylated in 2 cases (cases 3 and 35), whereas little methylation was found in the remaining 2 cases (cases 1 and 2). For further studies, we used methylation-specific PCR (MS-PCR) to detect DNA methylation in R region of 5′-LTR (Table I). DNA methylation in R region correlated with that in U3 region of 5′-LTR (data not shown). When 5′-LTR was completely methylated, only methylation band could be detected as shown in Figure 6 (lane 1), whereas only unmethylation band could be amplified if 5′-LTR was not methylated (lane 3). When 5′-LTR was partially methylated, both methylated and unmethylated bands were observed in ATL-55T (lane 2). In ATL-55T, the *tax* gene was transcribed, indicating that partial methylation of 5′-LTR could not silence the viral transcription. We analyzed DNA methylation of 5′-LTR in ATL cells except for them with type 2 defective provirus since they did not retain 5′-LTR. Among the ATL patients (28 cases), only methylation band could be detected in 5 cases (18%), and 5′-LTR was partially methylated in 14 cases (50%). However, it was not methylated in 9 cases (32%). Among 5 ATL cases in which only methylated bands were observed by MS-PCR, the *tax* gene transcript was observed only in a case (case 35). In this case, sodium bisulfite sequencing experiment revealed that the promoter-proximal TRE-1 was partially methylated, whereas CpG sites in the other 2 TRE-1s were completely methylated (Fig. 5). Since the promoter-proximal TRE-1 is critical for the viral transcription, partial methylation of TRE-1 is thought to allow the *tax* gene transcription. These data suggested that DNA methylation in 5′-LTR was implicated in silencing of *tax* gene expression; however, the complete DNA methylation of 5′-LTR associated with transcriptional suppression was not so frequent.

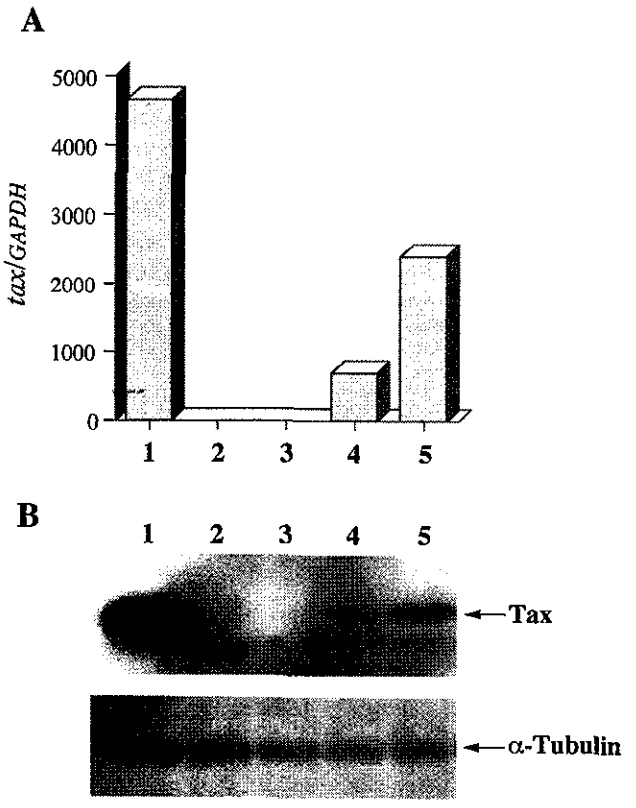

FIGURE 3 – Reactivation of *tax* gene transcripts after demethylation. ATL-43T, which retained the structure of *tax* gene, did not express *tax* gene transcript. After treatment with 5-Aza-CdR or with 5-Aza-CdR and Trichostatin A, *tax* gene transcripts were quantified by real-time PCR (*a*) and Tax proteins were detected using antibody against Tax (*b*). MT-4 was used as a positive control, and ED as a negative control. Lane 1, MT-4; lane 2, ED; lane 3, ATL-43T; lane 4, ATL-43T treated with 10 μM 5-Aza-CdR; lane 5, ATL-43T treated with 10 μM 5-Aza-CdR and 1 μM TSA.

Acetylation of histones H3 and H4 tails in the 5′-LTR of HTLV-I

The formation of the Tax/CREB complex on the HTLV-I promoter is critical for the recruitment of the co-activators CBP and p300. CBP/p300 have been shown to directly acetylate lysine residues within the amino-terminal tails of all 4 core histones.[34] Since the enhanced histone acetylation has been shown to correlate with activated transcription, we studied the acetylation of histones H3 and H4 in 5′-LTR of ATL cells with or without DNA methylation in this region by ChIP assay. Both histones were acetylated in ATL-55T cell (with partially methylated 5′-LTR) but not in ATL-43T cell (5′-LTR was hypermethylated as shown in Figs. 2 and 7). Since the transcription of *tax* gene was detected in ATL-55T, but not in ATL-43T, the levels of acetylation were coincident with the transcription of viral genes, which was consistent to the previous report.[35] We also studied the histone acetylation in 5′-LTR of the fresh ATL cell (case 1) without DNA methylation of 5′-LTR and detected hyper-acetylation of H3 and H4 histones, suggesting that the transcription of *tax* gene was active in ATL cells without DNA methylation of 5′-LTR *in vivo*. Indeed, the transcript of *tax* gene was detected in this case by RT-PCR (Table I). We could not study the acetylation of histones in ATL cells without DNA methylation and the *tax* gene transcription since such ATL cells were not available.

DISCUSSION

In certain virus-induced malignancies, cell lines established *in vitro* are quite different from the real neoplastic cells *in vivo*. For example, EBV can transform mature B-lymphocytes *in vitro*. In such cell lines, several viral genes are expressed, such as LMP, EBNA and EBER, which play important roles in such immortalization. However, viral genes are selectively expressed in Burkitt's lymphoma cells,[36] indicating that *in vivo* malignant cells are quite different from transformed cells *in vitro*. A similar phenomenon has been observed in HTLV-I associated cell lines. HTLV-I can transform CD4-positive T-lymphocytes *in vitro* in the presence of IL-2.[18] Such cell lines expressed Tax that was essential for immortalization as shown previously.[37] However, in the present study, we found Tax nonproducing cell lines, which were derived from leukemic cells, showing that Tax was not always essential for leukemogenesis. Furthermore, we identified the 3 different mechanisms in the inactivation of Tax production: nonsense mutation, deletion of *tax* gene and DNA methylation in of 5′-LTR.

Based on findings observed in ATL cell lines, we analyzed the *tax* gene and its expression in the fresh ATL cells. Expression of the *tax* gene in fresh ATL cells remains obscure in spite of extensive immunohistochemical and molecular studies.[14,38] In our study, we detected the *tax* gene transcripts in 14 of 41 cases (34%). Genetic changes, such as nonsense mutation, insertion and deletion of the *tax* gene, were also identified in the fresh ATL cells, which is consistent to the finding that ATL cell lines maintain leukemic state without Tax protein. Among ATL cases without the *tax* gene expression, we also showed selective DNA methylation of 5′-LTR as a mechanism involved in the suppression of the *tax* gene transcription. Recently, Koiwa *et al.*[39] reported that DNA methylation in 5′-LTR suppressed the expression of *tax* gene, suggesting its role in viral latency. It suggested the high frequency of DNA methylation of 5′-LTR. However, our study showed that complete methylation of 5′-LTR associated with loss of the *tax* gene transcription was not so frequent (4/28; 14%), and partial methylation of 5′-LTR was predominant in ATL cells (14/28; 50%). Since

TABLE I – MUTATIONS OF *TAX* GENES IN 47 ATL CASES[1]

Case number	ATL	Types of provirus	Methylation of 5'LTR	*tax*	*tax* expression
1	A	C	U	I	++
2	A	C	P	I	+
3	A	C	P	I	ND
4	A	C	ND	I	ND
5	A	C	U	I	–
6	A	C	P	I	+
7	A	C	P	I	+
8	A	C	M	I	–
9	A	C	P	I	–
10	A	C	P	I	–
11	A	C	P	I	++
12	A	C	U	I	–
13	A	C	P	I	–
14	A	C	M	I	–
15	A	C	P	**G7464A (W56*)**	+
16	A	C (multiple)	ND	G7464G/A (W56W/*)	–
17	A	C (multiple)	ND	I	ND
18	A	C (multiple)	ND	I	ND
19	A	DT1	U	I	–
20	A	DT1	U	**253 bp deletion**	++
21	A	DT1	P	**1 bp insertion**	ND
22	A	DT2	ND	I	–
23	A	DT2	ND	I	++
24	A	DT2	ND	I	–
25	A	DT2	ND	NA	ND
26	A	DT2	ND	NA	–
27	A	DT2	ND	NA	–
28	A	DT2	ND	NA	–
29	A	DT2	ND	G7346C (V17L)	–
30	A	DT2	ND	I	++
31	L	C	U	I	–
32	L	C	P	I	–
33	L	DT1	P	I	+
34	L	DT2	ND	NA	–
35	Ch	C	M	I	+
36	Ch	C	P	I	–
37	Ch	C	M	I	–
38	Ch	C	U	I	–
39	Ch	C	U	**G8040A (W248*)**	++
40	Ch	C (multiple)	ND	G7464G/A (W56W/*)	+
41	Ch	DT1	P	I	–
42	Ch	DT1	M	I	–
43	Ch	DT1	U	**G7464A (W56*), 8bp deletion**	–
44	Ch	DT2	ND	I	–
45	Ch	DT2	ND	I	+
46	Ch	DT2	ND	I	–
47	Ch	DT2	ND	I	–

[1]ND: not determined; NA: not amplified; I: intact; A: acute; L: lymphoma; Ch: chronic; C: complete provirus; DT1: defective type1; DT2: defective type2; M: methylated; U: unmethylated; P: partially methylated. Bold characters showed loss of expression of Tax.

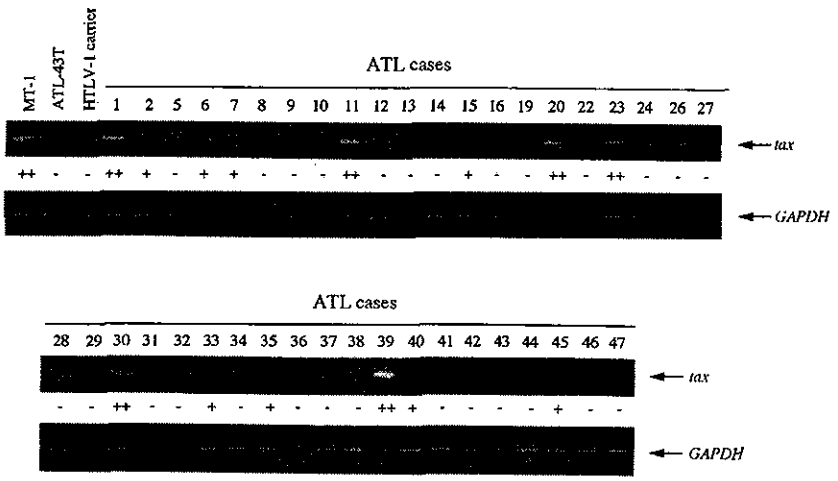

FIGURE 4 – Expression of *tax* gene in the PBMCs from ATL patients. The *tax* gene transcription was detected by RT-PCR (35 cycles), and *GAPDH* gene transcripts were amplified (25 cycles) as a control. The *tax* gene transcription was represented as high (++), low (+) and not detected (–). The numbering of cases corresponded to it in Table I.

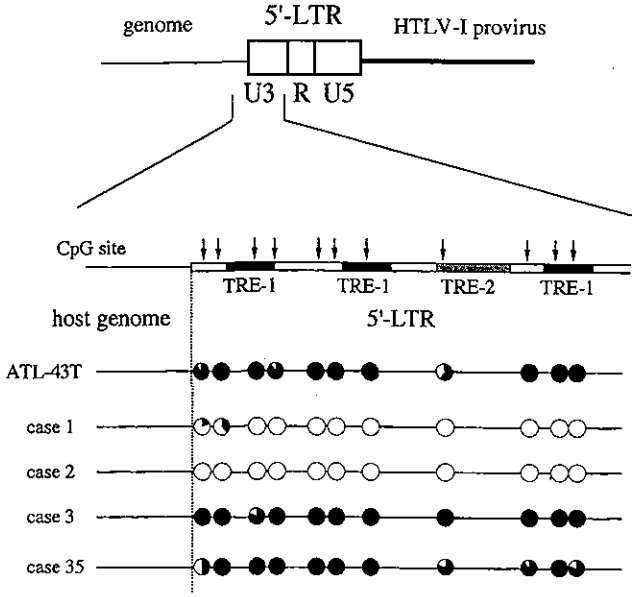

FIGURE 5 – DNA methylation of 5′-LTR in fresh ATL cells from 4 cases. DNA methylation was determined in 4 cases (cases 1, 2, 3 and 35 in Table I). PCR products from sodium bisulfite-treated genomic DNAs were subcloned into plasmid DNA, and the sequences of each 10 clones were determined. Each arrow showed a CpG site. Black portion represents the proportion of methylated CpG in each site.

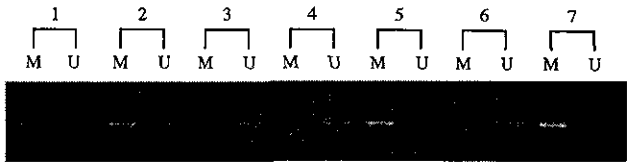

FIGURE 6 – DNA methylation of 5′-LTR detected by MS-PCR. DNA methylation of R region in 5′-LTR was detected by MS-PCR. Sodium bisulfite-treated DNA was amplified with each primer pair designed to detect the methylated (M) or unmethylated (U) 5′-LTR. Lane 1, ATL-43T (*tax* gene transcription (−) with completely methylated 5′-LTR); lane 2, ATL-55T (*tax* gene transcription (+) with partially methylated 5′-LTR); lane 3, ATL-48T (*tax* gene transcription (+) with unmethylated 5′-LTR); lane 4, case 1; lane 5, case 35; lane 6, case 2; lane 7,case 3.

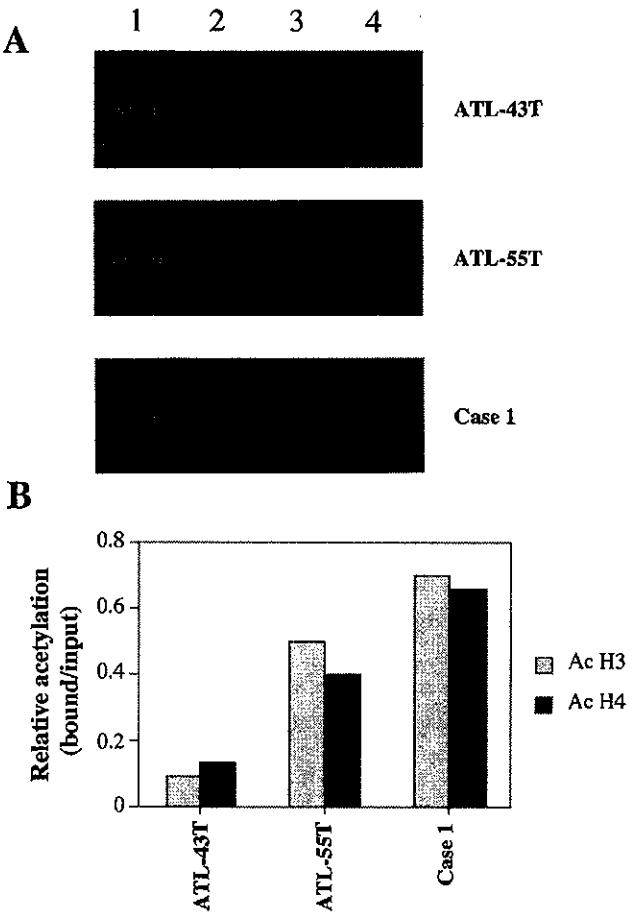

FIGURE 7 – Histone modification in 5′-LTR. (*a*) ChIP assay with antibody against acetylated histone H3 and H4. 1; input DNA, 2; control IgG, 3; anti-acetylated histone H3, 4; anti-acetylated histone H4. Experimental reactions were performed to determine optimal PCR conditions so that the yield of PCR products was dependent on the amount of input DNA (data not shown). (*b*) Quantification of relative acetylation levels. Values were calculated as relative signal intensity normalized by input DNA.

partial methylation of 5′-LTR did not silenced the *tax* gene transcription in both cell lines and fresh ATL cells, the transcriptional silencing by DNA methylation is not so common phenomenon. On the other hand, the *tax* gene transcript was detected in most fresh ATL cells with the genetically changed *tax* gene, which could not produce Tax protein. This finding also indicates that silencing of *tax* gene transcription is not necessary when Tax protein could not be produced, supporting the hypothesis that transcriptional silencing observed in ATL cells enables them to escape from the host immune system against Tax protein. Since the primary ATL cells did not express the *tax* gene transcripts (66%; 27 of 41 cases) even when 5′-LTR was unmethylated at all, it indicated that other mechanism than DNA methylation silenced the transcription of viral gene. Recent study showed that methylation of histone H3 lysine-9 is associated with silencing in the absence of DNA methylation, indicating that histone modification plays a critical role in the silencing of viral genes in HTLV-I infected cells.[40,41] The mechanism of such silencing should be clarified in the future study.

Such loss or suppression of Tax expression provided a significant clue to the leukemogenesis of ATL. The pleiotropic actions of Tax protein promoted proliferation and inhibited apoptosis of HTLV-I infected cells; however, at the same time, this protein was the major target of cytotoxic T-cells *in vivo*.[42–44] Thus, the presence of Tax in HTLV-I-infected cells provided advantages and disadvantages to the survival of HTLV-I-infected cells. It is speculated that Tax plays an important role in persistent proliferation of HTLV-I-infected cells during the carrier state, and then genetic and epigenetic changes accumulate in the host genome by mutator phenotype of Tax,[45] which finally lead to downregulation of Tax function and escape from the host immune system. Indeed, DNA methylation of 5′-LTR is less frequent in HTLV-I carriers compared to that of ATL cells (our unpublished data). DNA methylation and epigenetic changes of viral promoters down-regulate Tax expression and function, leading to escape from the host immune system.

We previously identified the type 2 defective provirus that lacked 5′-LTR and internal sequences such as *gag* and *pol*, in ATL cells.[15] The U3 region of 5′-LTR contains the critical motifs for transcription of viral genes and DNA methylation associated with histone deacetylation of this region are thought to disturb the interaction with various transcriptional factors including CREB, ATF-1, ATF-2 and other members of CREB-ATF superfamily transcriptional factors,[30,32,35] resulting in silencing of viral transcription. In our study, deletion of 5′-LTR was identified in 30%

of fresh ATL cases. The presence of internal promoter in the *pol* region has been reported in HTLV-I,[46] which might cause the transcription of *tax* gene without 5′-LTR. However, 5 of our 14 ATL cases with type 2 defective provirus also lacked the internal promoter and the second exon of *tax* gene. In such cases without 5′-LTR and internal promoter, the *tax* gene transcription could not be detected. However, the *tax* gene was transcribed in 3 cases with type 2 defective provirus, indicating that internal promoter or trapped cellular promoter was responsible for such *tax* gene transcription. Taken together, loss of 5′-LTR could not abolish the *tax* gene transcription, but diminish that.

In conclusion, we show that genetic and epigenetic changes of viral promoters attenuate Tax expression and function, which is considered to enable ATL cells to escape from host immune system. Further studies are necessary to clarify the epigenetic mechanism to silence the *tax* gene transcription.

ACKNOWLEDGMENTS

We thank M. Fujii for valuable suggestions. KN is a Research Fellow of the Japan Society for the Promotion of Science.

REFERENCES

1. Takatsuki K, Uchiyama T, Sagawa K, Yodoi J. Adult T cell leukemia in Japan. In: Seno S, Takaku F, Irino S, eds. Topic in hematology, the 16th International Congress of Hematology. Amsterdam, 1977. 73–77.
2. Uchiyama T, Yodoi J, Sagawa K, Takatsuki K, Uchino H. Adult T-cell leukemia: clinical and hematologic features of 16 cases. Blood 1977;50:481–92.
3. Poiesz BJ, Ruscetti FW, Gazdar AF, Bunn PA, Minna JD, Gallo RC. Detection and isolation of type C retrovirus particles from fresh and cultured lymphocytes of a patient with cutaneous T-cell lymphoma. Proc Natl Acad Sci U S A 1980;77:7415–9.
4. Wong-Staal F, Gallo RC. Human T-lymphotropic retroviruses. Nature 1985;317:395–403.
5. Seiki M, Hattori S, Hirayama Y, Yoshida M. Human adult T-cell leukemia virus: complete nucleotide sequence of the provirus genome integrated in leukemia cell DNA. Proc Natl Acad Sci U S A 1983; 80:3618–22.
6. Takatsuki K, Yamaguchi K, Matsuoka M. ATL and HTLV-I-related diseases. In: Takatsuki K, ed. Adult T-cell leukemia New York: Oxford University Press, 1994. 1–27.
7. Arisawa K, Soda M, Endo S, Kurokawa K, Katamine S, Shimokawa I, Koba T, Takahashi T, Saito H, Doi H, Shirahama S. Evaluation of adult T-cell leukemia/lymphoma incidence and its impact on non-Hodgkin lymphoma incidence in southwestern Japan. Int J Cancer 2000;85:319–24.
8. Matsuoka M. Adult T-cell leukemia/Lymphoma. In: Goedert JJ, ed. Infectious Causes of Cancer. Totowa: Humana Press, 2000. 221–29.
9. Franchini G. Molecular mechanisms of human T-cell leukemia/lymphotropic virus type I infection. Blood 1995;86:3619–39.
10. Yoshida M. Multiple viral strategies of htlv-1 for dysregulation of cell growth control. Annu Rev Immunol 2001;19:475–96.
11. Jin DY, Spencer F, Jeang KT. Human T cell leukemia virus type I oncoprotein Tax targets the human mitotic checkpoint protein MAD1. Cell 1998;93:81–91.
12. Suzuki T, Uchida-Toita M, Yoshida M. Tax protein of HTLV-1 inhibits CBP/p300-mediated transcription by interfering with recruitment of CBP/p300 onto DNA element of E-box or p53 binding site. Oncogene 1999;18:4137–43.
13. Ariumi Y, Kaida A, Lin JY, Hirota M, Masui O, Yamaoka S, Taya Y, Shimotohno K. HTLV-1 tax oncoprotein represses the p53-mediated trans-activation function through coactivator CBP sequestration. Oncogene 2000;19:1491–9.
14. Franchini G, Wong-Staal F, Gallo RC. Human T-cell leukemia virus (HTLV-I) transcripts in fresh and cultured cells of patients with adult T-cell leukemia. Proc Natl Acad Sci U S A 1984;81:6207–11.
15. Tamiya S, Matsuoka M, Etoh K, Watanabe T, Kamihira S, Yamaguchi K, Takatsuki K. Two types of defective human T-lymphotropic virus type I provirus in adult T-cell leukemia. Blood 1996;88:3065–73.
16. Furukawa Y, Kubota R, Tara M, Izumo S, Osame M. Existence of escape mutant in HTLV-I tax during the development of adult T-cell leukemia. Blood 2001;97:987–93.
17. Katoh T, Harada T, Morikawa S, Wakutani T. IL-2- and IL-2-R-independent proliferation of T-cell lines from adult T-cell leukemia/lymphoma patients. Int J Cancer 1986;38:265–74.
18. Maeda M, Shimizu A, Ikuta K, Okamoto H, Kashihara M, Uchiyama T, Honjo T, Yodoi J. Origin of human T-lymphotrophic virus I-positive T cell lines in adult T cell leukemia. Analysis of T cell receptor gene rearrangement. J Exp Med 1985;162:2169–74.
19. Maeda M, Arima N, Daitoku Y, Kashihara M, Okamoto H, Uchiyama T, Shirono K, Matsuoka M, Hattori T, Takatsuki K. Evidence for the interleukin-2 dependent expansion of leukemic cells in adult T cell leukemia. Blood 1987;70:1407–11.
20. Nosaka K, Maeda M, Tamiya S, Sakai T, Mitsuya H, Matsuoka M. Increasing methylation of the CDKN2A gene is associated with the progression of adult T-cell leukemia. Cancer Res 2000;60:1043–8.
21. Shimoyama M. Diagnostic criteria and classification of clinical subtypes of adult T-cell leukaemia-lymphoma: a report from the Lymphoma Study Group (1984–87). Br J Haematol 1991;79:428–37.
22. Lee B, Tanaka Y, Tozawa H. Monoclonal antibody defining Tax1 protein of human T-cell leukemia virus type-I. Tohoku J Exp Med 1989;157:1–11.
23. Etoh K, Tamiya S, Yamaguchi K, Okayama A, Tsubouchi H, Ideta T, Mueller N, Takatsuki K, Matsuoka M. Persistent clonal proliferation of human T-lymphotropic virus type I-infected cells in vivo. Cancer Res 1997;57:4862–7.
24. Herman JG, Graff JR, Myohanen S, Nelkin BD, Baylin SB. Methylation-specific PCR: a novel PCR assay for methylation status of CpG islands. Proc Natl Acad Sci U S A 1996;93:9821–6.
25. Yasunaga J, Sakai T, Nosaka K, Etoh K, Tamiya S, Koga S, Mita S, Uchino M, Mitsuya H, Matsuoka M. Impaired production of naive T lymphocytes in human T-cell leukemia virus type I-infected individuals: its implications in the immunodeficient state. Blood 2001;97: 3177–83.
26. Nguyen CT, Gonzales FA, Jones PA. Altered chromatin structure associated with methylation-induced gene silencing in cancer cells: correlation of accessibility, methylation, MeCP2 binding and acetylation. Nucleic Acids Res 2001;29:4598–606.
27. Brady J, Jeang KT, Duvall J, Khoury G. Identification of p40x-responsive regulatory sequences within the human T-cell leukemia virus type I long terminal repeat. J Virol 1987;61:2175–81.
28. Fujisawa J, Seiki M, Sato M, Yoshida M. A transcriptional enhancer sequence of HTLV-I is responsible for trans-activation mediated by p40 chi HTLV-I. Embo J 1986;5:713–8.
29. Marriott SJ, Lindholm PF, Brown KM, Gitlin SD, Duvall JF, Radonovich MF, Brady JN. A 36-kilodalton cellular transcription factor mediates an indirect interaction of human T-cell leukemia/lymphoma virus type *I TAX1* with a responsive element in the viral long terminal repeat. Mol Cell Biol 1990;10:4192–201.
30. Datta S, Kothari NH, Fan H. In vivo genomic footprinting of the human T-cell leukemia virus type 1 (HTLV-1) long terminal repeat enhancer sequences in HTLV-1-infected human T-cell lines with different levels of Tax I activity. J Virol 2000;74:8277–85.
31. Cameron EE, Bachman KE, Myohanen S, Herman JG, Baylin SB. Synergy of demethylation and histone deacetylase inhibition in the re-expression of genes silenced in cancer. Nat Genet 1999;21:103–7.
32. Datta S, Kothari NH, Fan H. Induction of Tax i expression in MT-4 cells by 5-azacytidine leads to protein binding in the HTLV-1 LTR in vivo. Virology 2001;283:207–14.
33. Saggioro D, Panozzo M, Chieco-Bianchi L. Human T-lymphotropic virus type I transcriptional regulation by methylation. Cancer Res 1990;50:4968–73.
34. Ogryzko VV, Schiltz RL, Russanova V, Howard BH, Nakatani Y. The transcriptional coactivators p300 and CBP are histone acetyltransferases. Cell 1996;87:953–9.
35. Lemasson I, Polakowski NJ, Laybourn PJ, Nyborg JK. Transcription factor binding and histone modifications on the integrated proviral promoter in human T-cell leukemia virus-I-infected T-cells. J Biol Chem 2002;277:49459–65.
36. de The G. Epstein-Barr virus and Burkitt's lymphoma Goedert, J.J. Totowa: Humana Press, 2000. 77–92.
37. Grassmann R, Berchtold S, Radant I, Alt M, Fleckenstein B, Sodroski JG, Haseltine WA, Ramstedt U. Role of human T-cell leukemia virus type 1 X region proteins in immortalization of primary human lymphocytes in culture. J Virol 1992;66:4570–5.
38. Ohshima K, Suzumiya J, Izumo S, Mukai Y, Tashiro K, Kikuchi M. Detection of human T-lymphotropic virus type-I DNA and mRNA in the lymph nodes; using polymerase chain reaction in situ hybridization (PCR/ISH) and reverse transcription (RT-PCR/ISH). Int J Cancer 1996;66:18–23.
39. Koiwa T, Hamano-Usami A, Ishida T, Okayama A, Yamaguchi K, Kamihira S, Watanabe T. 5′-Long terminal repeat-selective cpg methylation of latent human t-cell leukemia virus type 1 provirus in vitro and in vivo. J Virol 2002;76:9389–97.

40. Pannell D, Osborne CS, Yao S, Sukonnik T, Pasceri P, Karaiskakis A, Okano M, Li E, Lipshitz HD, Ellis J. *Retrovirus vector* silencing is de novo methylase independent and marked by a repressive histone code. Embo J 2000;19:5884–94.
41. Bachman KE, Park BH, Rhee I, Rajagopalan H, Herman JG, Baylin SB, Kinzler KW, Vogelstein B. Histone modifications and silencing prior to DNA methylation of a tumor suppressor gene. Cancer Cell 2003;3:89–95.
42. Jacobson S, Shida H, McFarlin DE, Fauci AS, Koenig S. Circulating CD8+ cytotoxic T lymphocytes specific for HTLV-I pX in patients with HTLV-I associated neurological disease. Nature 1990;348:245–8.
43. Kannagi M, Harada S, Maruyama I, Inoko H, Igarashi H, Kuwashima G, Sato S, Morita M, Kidokoro M, Sugimoto M, Funabashi S, Osame M, et al. Predominant recognition of human T cell leukemia virus type I (HTLV-I) pX gene products by human CD8+ cytotoxic T cells directed against HTLV- I-infected cells. Int Immunol 1991;3:761–7.
44. Hanon E, *Hall S, Taylor GP, Saito M*, Davis R, Tanaka Y, Usuku K, Osame M, Weber JN, Bangham CR. Abundant tax protein expression in CD4+ T cells infected with human T-cell lymphotropic virus type I (HTLV-I) is prevented by cytotoxic T lymphocytes. Blood 2000;95: 1386–92.
45. Jin DY, Giordano V, Kibler KV, Nakano H, Jeang KT. Role of adapter function in oncoprotein-mediated activation of NF-kappaB. Human T-cell leukemia virus type I Tax interacts directly with IkappaB kinase gamma. J Biol Chem 1999;274:17402–5.
46. Ariumi Y, Shimotohno K, Noda M, Hatanaka M. Characterization of the internal promoter of human T-cell leukemia virus type I. FEBS Lett 1998;423:25–30.

Leukemia (2004) 18, 1357–1363

www.nature.com/leu

MOLECULAR TARGETS FOR THERAPY

Proteasome inhibitor, bortezomib, potently inhibits the growth of adult T-cell leukemia cells both *in vivo* and *in vitro*

Y Satou[1], K Nosaka[1], Y Koya[1], J-i Yasunaga[1], S Toyokuni[2] and M Matsuoka[1]

[1]*Institute for Virus Research, Kyoto University, Kyoto, Japan; and* [2]*Department of Pathology and Biology of Diseases, Graduate School of Medicine, Kyoto University, Kyoto, Japan*

Adult T-cell leukemia (ATL) is a fatal neoplasm derived from CD4-positive T-lymphocytes, and regardless of intensive chemotherapy, its mean survival time is less than 1 year. Nuclear factor-κB (NF-κB) activation was reported in HTLV-I associated cells, and has been implicated in oncogenesis and resistance to anticancer agents and apoptosis. We studied the effect of a proteasome inhibitor, bortezomib (formerly known as PS-341), on ATL cells *in vitro* and *in vivo*. Bortezomib could inhibit the degradation of IκBα in ATL cells, resulting in suppression of NF-κB and induction of cell death in ATL cells *in vitro*. Susceptibilities to bortezomib were well correlated with NF-κB activation, suggesting that suppression of the NF-κB pathway was implicated in the cell death induced by bortezomib. Although the majority of the cell death was apoptosis, necrotic cell death was observed in the presence of a caspase inhibitor, z-VAD-fmk. When bortezomib was administered into SCID mice bearing tumors, it suppressed tumor growth *in vivo*, showing that bortezomib was effective against ATL cells *in vivo*. These studies revealed that bortezomib is highly effective against ATL cells *in vitro* and *in vivo* by induction of apoptosis, and its clinical application might improve the prognosis of patients with this fatal disease.
Leukemia (2004) **18**, 1357–1363. doi:10.1038/sj.leu.2403400
Published online 10 June 2004
Keywords: ATL; HTLV-I; proteasome inhibitor; NF-κB; apoptosis

Introduction

Adult T-cell leukemia (ATL) has been established as a distinct clinical entity based on the clinical features and geographic distribution of patients.[1,2] Although G-CSF-supported combination chemotherapy improved the survival (mean survival time, 13 months),[3] the prognosis of aggressive ATL remains poor, with death usually occurring due to opportunistic infections or drug resistance.[4,5] Therefore, development of anticancer drugs designed to overwhelm the resistance of ATL cells is urgently needed.

Tax is a 40-kDa protein encoded by the pX region in the human T-cell leukemia virus type (HTLV-I) genome, and is thought to play a central role in the leukemogenesis of ATL through its pleiotropic actions.[6] Tax can activate not only the transcription of viral genes but also that of a number of cellular genes through several distinct transcription factors. Tax can activate the nuclear factor-κB (NF-κB) pathway through direct interaction with IKKγ. IKKα, β and γ form a 700 kDa complex, in which IKKγ functionally adapts Tax into the large complex.[7] The activated complex causes IκBα to be phosphorylated, ubiquitylated, and subsequently degraded by proteasomes.[8] The degradation of IκBα allows NF-κB proteins to translocate into the nucleus and bind their DNA-binding sites to activate the transcription of target genes, including cytokines, chemokines, stress-response genes, and antiapoptotic genes. On the other hand, ATL cells without Tax expression also exhibited the activated NF-κB pathway, although its mechanism remains unknown.[9]

Proteasome inhibitors are novel antitumor agents with preclinical evidence of activity against hematological malignancies and solid tumors.[10,11] Among them, a boronic acid dipeptide with selective activity as a proteasome inhibitor, bortezomib, is the first proteasome inhibitor to be approved for clinical use.[10,12] Although numerous molecular targets of proteasome inhibitors have been proposed,[13] one of the mechanisms is that inhibition of the proteasome abrogates degradation of IκBs induces their cytoplasmic accumulation, which blocks the nuclear translocation and transcriptional activity of NF-κB. This effect may account in part for the antitumor effect of bortezomib. From this point of view, suppression of the NF-κB pathway by bortezomib might be useful as a therapy against ATL.

In this study, we investigated the antitumor effects of bortezomib on HTLV-I-infected cell lines *in vitro* and *in vivo*, and primary ATL cells *in vitro*. The findings of this study that bortezomib exhibited antitumor activities towards ATL cells both *in vitro* and *in vivo* suggest a clinical potential for treatment of this fatal disease, ATL.

Materials and methods

Cells

In all, 10 HTLV-I associated cell lines were used in the present study: ED(−), ATL-43Tb(−), ATL-55T(+), TL-Om1, Sez627, ATL-35T, MT-1, MT-2, MT-4, and Hut102.[14,15] Four HTLV-I nonassociated T-cell lines, Jurkat, Sup-T1, CEM, and Hut78, were used as controls. After informed consent, peripheral blood mononuclear cells (PBMCs) were isolated from patients with acute ATL by Ficoll-Hypaque.

Drugs

The proteasome inhibitor, bortezomib (kindly provided by Millennium Pharmaceuticals, Cambridge, MA, USA), was

Correspondence: Dr M Matsuoka, Institute for Virus Research, Kyoto University, 53 Shogoin Kawahara-cho, Sakyo-ku, Kyoto 606-8506, Japan; Fax: +81 75 751 4049; E-mail: mmatsuok@virus.kyoto-u.ac.jp
Received 19 September 2003; accepted 23 April 2004; Published online 10 June 2004

dissolved in DMSO and stored at −20°C until use. For *in vivo* experiments, we used bortezomib mixed with mannitol to increase solubility. Anti-Fas mAb, CH11, and z-VAD-fmk were purchased from MBL (Nagoya, Japan), and the PEPTIDE INSTITUTE INC (Osaka, Japan).

MTT assay

The inhibitory effects of bortezomib on cell growth were assessed by measuring the 3-(4,5-dimethylthiazol-2-yl)-2,5-diphenyl tetrazolium bromide (MTT) dye absorbance of the cells.

Measurement of apoptotic cell death

For detection of apoptosis, the Annexin V-binding capacities of the treated cells were examined by flow cytometry using an Annexin V-FITC Apoptosis Detection Kit (MBL, Nagoya, Japan), according to the manufacturer's instructions. For fresh ATL cells, the percentages of specific apoptosis were calculated as follows: % specific apoptosis = (Annexin V positivity−spontaneous Annexin V positivity)/(100−spontaneous Annexin V positivity) × 100. To detect DNA fragmentation by the TUNEL assay, we used a MEBSTAIN Apoptosis Kit Direct (MBL) (see supplemental information).

Evaluation of NF-κB activity

The nuclear extracts were prepared as reported previously. The DNA-binding activity of NF-κB in the HTLV-I associated cell lines was quantified by enzyme-linked immunosorbent assay (ELISA) using a Trans-AM™ NF-κB p65 Transcription Factor Assay Kit (Active Motif North America, Carlsbad, CA, USA), according to the manufacturer's instructions (see supplemental information).

Immunoblotting

Western blot was performed as described previously, with primary antibodies against IκBα or α-tubulin (Santa Cruz Biotechnology, Santa Cruz, CA, USA), or Tax (MI-73).[16] The membranes were washed in 0.5% TPBS, and incubated with the secondary antibody, HRP-conjugated anti-rabbit IgG or anti-mouse IgG (Santa Cruz Biotechnology), followed by visualization of the proteins by enhanced chemiluminescence films (Amersham Pharmacia Biotech, Buckinghamshire, UK) and a reagent (Santa Cruz Biotechnology). The intensities of the IκBα bands were quantified using ATTO densitograph 4.0 (ATTO, Tokyo, Japan).

Morphological evaluation by electron microscopy

For observation by transmission electron microscopy, ED(−) cells (4×10^7), which were cultured with or without bortzomib, were fixed in 2% glutaraldehyde (Nacalai Tesque) in 0.1 M phosphate-buffered saline, and observed with a Hitachi H-7000 electron microscope (Hitachi, Tokyo, Japan) as reported previously.[17]

Xenograft murine model

Immune-deficient SCID (C.B-17/Icr-scidJcl) mice were inoculated subcutaneously into the right flank with ED cells (4×10^7/mouse) in 200 μl of RPMI. When the tumors became measurable, mice were assigned into the treatment group receiving bortezomib or the control group. Treatment with bortezomib (1.0 mg/kg) was given i.p. twice a week. The sizes of the subcutaneous tumors were measured every 2 days and recorded as the longest surface length (*a* (in mm)) and width (*b* (in mm)). The tumor volume (*V* (in m^3)) was then calculated according to the following formula: $V = a \times b^2 \times 0.5$. Animals were killed when their tumors reached 2 cm or when the mice became moribund.

Statistical analysis

The EC_{50}s of bortezomib against the different cell lines were studied by the nonparametric Mann–Whitney *U* test. The differences in NF-κB activation between HTLV-I associated cell lines and nonassociated T-cell lines, and IκBα expression between Tax-expressing and nonexpressing cell lines were statistically analyzed using Welch's *t*-test. A *P*-value less than 0.05 denoted a statistically significant difference. The correlation between the EC_{50} of bortezomib and NF-κB activation was analyzed by the Spearman's correlation coefficient by the rank test.

Results

Bortezomib induced cell death of HTLV-I associated cell lines

First, we investigated the *in vitro* effects of bortezomib on HTLV-I associated and nonassociated T-cell lines by MTT assays. Although the sensitivity to bortezomib varied among the cell lines studied, HTLV-I associated cell lines were more susceptible to bortezomib than HTLV-I nonassociated T-cell lines (Table 1) ($P = 0.024$, Mann–Whitney). Two types of HTLV-I cell

Table 1 Sensitivity to bortezomib in various T-cell lines

HTLV-I	Tax status	Cell line	IC_{50} (nM)[a]	
+	+[b]	MT-2	5.2±0.7	
+	+	MT-4	4.3±0.7	
+	+	Sez627	13.9±2.8	
+	+	HUT-102	4.6±0.1	
+	+	ATL-35T	4.3±0.5	$p = 0.116$
+	-*[c]	MT-I	5.6±0.9	
+	-	43Tb(-)	8.0±4.0	
+	-	ED(-)	9.1±4.4	
+	-	ATL-55T(+)	4.9±1.1	
+	-	TL-Om1	38.9±5.8	$p = 0.024$
-	-	CEM	18.6±5.9	
-	-	Jurkat	23.2±2.8	
-	-	Hut78	34.0±10.0	
-	-	Sup-T1	24.5±10.0	
-	-	PBMC	>100	
-	-	PHA-blast	63.9±30.5	

[a]Values are means ± 1 s.d. of triplicate determination.
[b]+Tax expression can be detected by Western blotting.
[c]*Tax expression cannot be detected by Western blotting, but can be detected by RT-PCR.

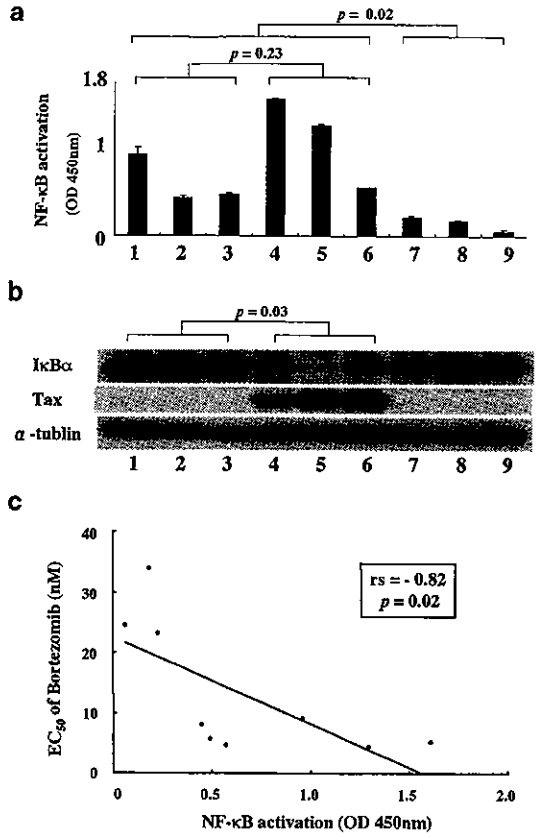

Figure 1 NF-κB binding activity, and expressions of IκBα and Tax in various T-cell lines. (a) To determine NF-κB binding activity, nuclear extracts (2 μg per well) from various cells were analyzed using a Trans-AM™ NF-κB p65 Transcription Factor Assay Kit (Active Motif North America), according to the manufacturer's instructions. Lane 1, ED(−); Lane 2, ATL-43Tb(−); Lane 3, MT-1; Lane 4, MT-2; Lane 5, MT-4; Lane 6, HUT102; Lane 7, Jurkat; Lane 8, Hut78; Lane 9, SupT1. (b) Whole-cell extracts (30 μg per lane) of various T-cell lines were immunoblotted with specific antibodies against IκBα, Tax, and α-tubulin. The indicated lanes are identical in Figure 1a. (c) The correlation between NF-κB activation and the EC_{50}s of bortezomib in various T-cell lines was determined by Spearman's rank test.

lines were reported with respect to Tax expression: Tax-expressing (Figure 1b, lanes 4–6) and Tax nonexpressing (lanes 1–3) cell lines. Most of the HTLV-I-infected cell lines without Tax expression were derived from the leukemic cells identified *in vivo*.[14] On the other hand, HTLV-I-infected cell lines that were established *in vitro* or HTLV-I cell lines derived from nonleukemic cells usually expressed Tax protein. Although Tax expression was reported to be associated with resistance against apoptosis,[18] it did not influence the susceptibility to bortezomib among the HTLV-I associated cell lines ($P=0.116$, Mann–Whitney).

Bortezomib inhibits NF-κB activation of HTLV-I associated cell lines

Constitutive activation of the NF-κB pathway was previously reported in HTLV-I associated cell lines, and has been shown to be critical for the proliferation and inhibition of apoptosis in Tax-expressing cells.[6,7] Although Tax protein can activate NF-κB by enhanced degradation of IκB, ATL cells without Tax expression also showed the activated NF-κB.[9] In order to study the NF-κB activity in HTLV-I associated cell lines, the DNA-binding activity of NF-κB was quantified by an ELISA assay as described. As shown in Figure 1a, HTLV-I associated cell lines exhibited the constitutive activation of NF-κB, which was statistically significant in HTLV-I associated cell lines compared with other T-cell lines ($P=0.02$, Welch's *t*-test). To confirm the specificity of the assay, we used two oligonucleotides provided as a competitor for NF-κB binding. Wild-type consensus oligonucleotides could prevent NF-κB binding to the probe immobilized on the plate. Conversely, the mutated consensus oligonucleotide had no effect on DNA binding (data not shown).

Previous studies have shown that Tax binds to IKKγ/NEMO, resulting in enhanced degradation of IκBα, and activation of NF-κB in Tax-expressing cell lines.[19,20] Therefore, we next analyzed the protein levels of IκBα and Tax. The IκBα protein was statistically more decreased in Tax-expressing cell lines than in Tax nonexpressing cell lines ($P=0.027$, Welch's *t*-test) (Figure 1b). However, the NF-κB activations did not differ between Tax-expressing and nonexpressing HTLV-I associated cell lines ($P=0.23$, Welch's *t*-test).

Since the higher activation of NF-κB and increased susceptibility to bortezomib in HTLV-I associated cell lines suggested their association, we analyzed the correlation between NF-κB activation and susceptibility to bortezomib. Indeed, the EC_{50}s of T- cell lines were inversely correlated with the activation of NF-κB ($rs=-0.817$, Spearman's correlation coefficient by rank test) (Figure 1c). From this result, the enhanced activation of NF-κB was associated with increased susceptibility to bortezomib among the HTLV-I associated cell lines.

In order to clarify the effect of bortezomib, we analyzed the NF-κB activity and protein level of IκBα in ED(−) (Tax-negative) and MT-4 (Tax-positive) cells after treatment with bortezomib. As shown in Figure 2a, bortezomib inhibited the NF-κB activation in both ED(−) and MT-4 cells in a time-dependent manner. Consistent with the decreased activity of NF-κB, bortezomib induced the accumulation of both IκBα and the slower migrating form of phosphorylated IκBα in MT-4 cells (Figure 2b). On the other hand, bortezomib increased only phosphorylated IκBα in ED(−) cells, suggesting that the increment of phosphorylated IκBα was associated with the inhibition of NF-κB. In addition, bortezomib did not influence the expression of Tax protein in either ED(−) or MT-4 cells, which showed that Tax was not the target of the proteasome inhibitor.

Bortezomib induced both apoptotic and nonapoptotic cell death

To study whether the cell death induced by bortezomib was apoptosis, we analyzed the bortezomib-induced cell death by the TUNEL method. Bortezomib induced apoptosis in ED(−) (60.6%) and MT-4 (77.9%) cells (supplemental Figure 1a), indicating that most of the cell deaths induced by bortezomib was apoptosis, as has been observed in other cancers. However, the pan-caspase inhibitor, z-VAD-fmk, that inhibits caspases 1, 3, 4, 7 and 8, did not inhibit the cell death of ED(−) cells after treatment with bortezomib, whereas it suppressed the Fas-mediated cell death (Figure 3a). As shown in Figure 3b, z-VAD-fmk completely blocked the apoptosis induced by bortezomib whereas cell death estimated by PI and Annexin V staining was still detected in 75.7% of cells, suggesting that the cell death induced by bortezomib in the presence of z-VAD-fmk might not be apoptotic. Moreover, z-VAD-fmk could not block the loss of

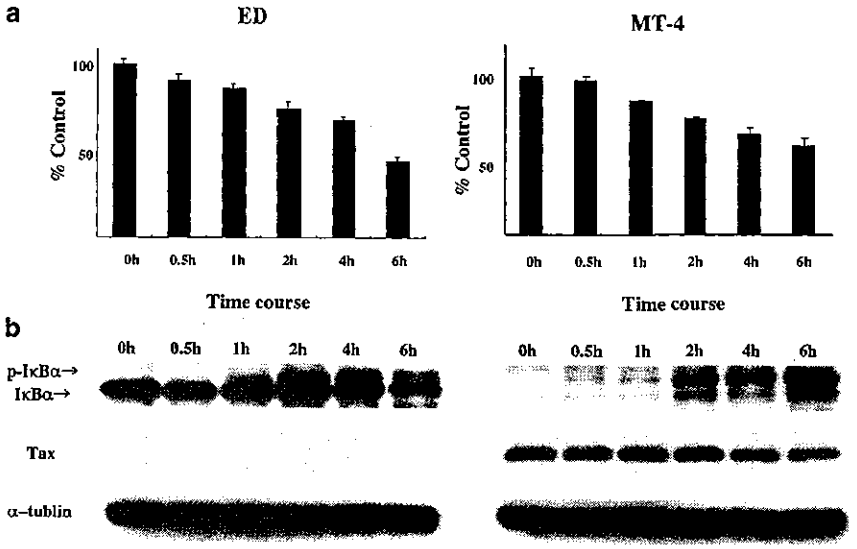

Figure 2 Bortezomib induced the accumulation of phosphorylated IκBα and inhibited NF-κB activity. (a) ED(−) and MT-4 cells were treated with bortezomib (100 nM) for the indicated times, followed by nuclear extraction. NF-κB activities of nuclear extracts (2 μg per well) at the indicated times were quantified using a Trans-AM™ NF-κB p65 Transcription Factor Assay Kit (Active Motif North America), according to the manufacturer's instructions. (b) ED(−) and MT-4 cells were treated with bortezomib (100 nM) for the indicated times, followed by protein extraction. Whole-cell extracts (30 μg per lane) of treated cells were immunoblotted with specific antibodies against IκBα, Tax, and α-tubulin.

mitochondrial transmembrane potential, an initial and irreversible apoptotic change in mitochondria, induced by bortezomib in the presence of z-VAD-fmk (supplemental Figure 1b). To confirm that cell death was induced by bortezomib in the presence of z-VAD-fmk, the bortezomib treated cells were studied by transmission electron microscopy. Treatment of bortezomib alone caused condensation and fragmentation of the nuclei as well as shrinkage of the cells (Figure 4b), which are characteristics of apoptosis. When the cells were treated with bortezomib in the presence of z-VAD-fmk, their cytoplasms appeared electron translucent accompanied by cellular swelling and their mitochondrial matrices were swollen (Figure 4c and d), which were characteristics of necrosis. These findings indicated that although bortezomib induced apoptosis, it induced necrosis in the presence of z-VAD-fmk.

Antitumor activity of bortezomib in vivo

Since bortezomib was found to rapidly exit the plasma compartment,[10] we analyzed the *in vivo* effects of bortezomib on ATL cells. A previous report showed that bortezomib monotherapy was not effective in a murine ATL model although it has the ability to enhance anti-Tac activity.[21] We used ED(−) cells derived from leukemic cells in an ATL patient. As shown in Figure 5, the treatment with bortezomib (1 mg/kg) alone significantly inhibited the growth of ED(−) cells *in vivo* without the obvious adverse effects. This result indicated that bortezomib monotherapy was effective against ED(−) cells *in vivo*.

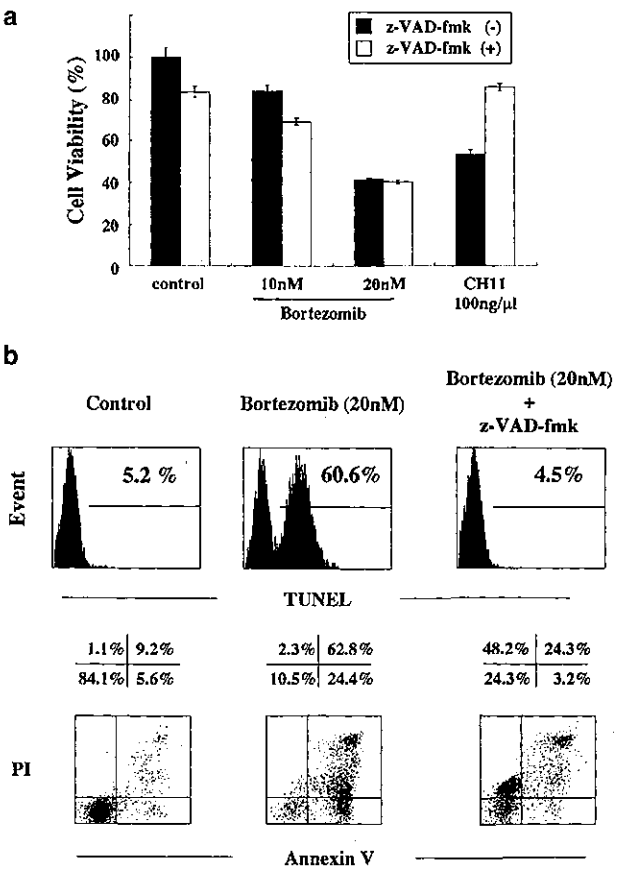

Figure 3 Bortezomib induced cell death in HTLV-I associated cell lines. (a) The cytotoxic activities of bortezomib and CH11 were measured by MTT assays with or without the pan-caspase inhibitor, z-VAD-fmk (10 μM). ED(−) cells were cultured in the presence of the indicated drugs for 48 h. The percentages of viable cells are shown with respect to untreated cells. The data shown are the means and ranges of triplicate cultures. (b) ED(−) cells were cultured in the presence of the indicated drugs for 24 h. Cell death was analyzed by Annexin V-PI staining and the TUNEL method. The percentages of each fraction are shown.

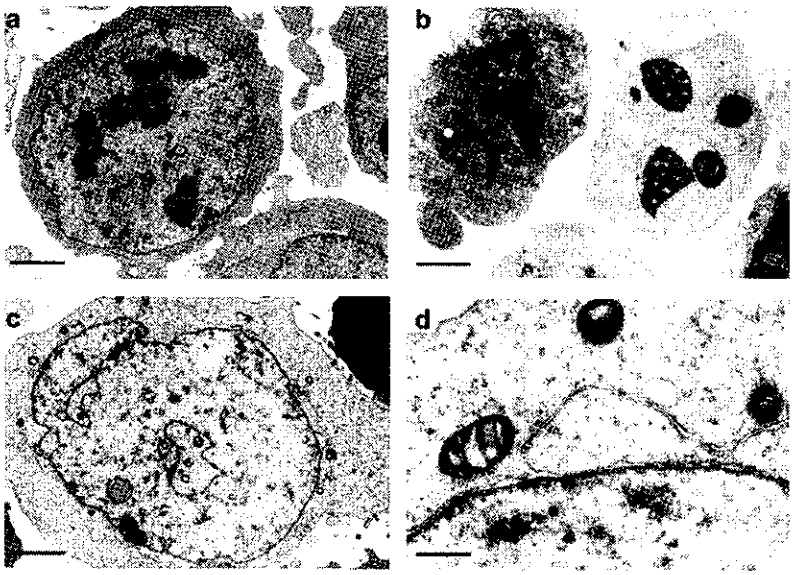

Figure 4 Apoptotic and necrotic cell death induced by bortezomib. (a) As control, untreated cells are shown. (b) ED(−) cells were treated with 20 nM bortezomib for 12 h. That caused condensation and fragmentation of the nuclei as well as shrinkage of the cells, which are characteristics of apoptosis. (c, d) ED(−) cells were treated with 20 nM bortezomib in the presence of 10 μM z-VAD-fmk for 18 h. Their cytoplasm appeared electron translucent accompanied by cellular swelling and their mitochondrial matrices were swollen, which were characteristic changes of necrotic cell death. Bars represent 8 μm (a–c) and 1.25 μm (d).

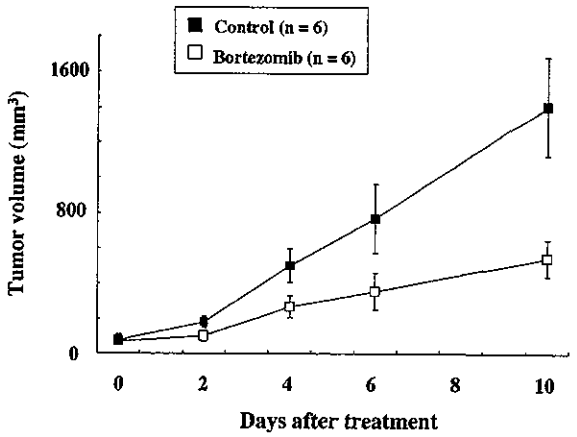

Figure 5 Antitumor efficacy of bortezomib against ATL-derived cell line ED(−) xenografts in SCID mice. ED(−) cells were injected subcutaneously into the right flanks (4×10^7 cells/mouse) of 5-week-old female SCID mice. When the tumor size became measurable, animals were treated intraperitoneally twice a week with either vehicle or bortezomib for 10 days. Tumor volumes were determined as described in the Materials and Methods, and are presented as the average values and s.d. of six mice.

Effect of bortezomib on primary ATL cells

Lastly, we studied the effect of bortezomib against primary ATL cells. Bortezomib induced the apoptosis of fresh ATL cells, although there were some differences among cases (supplemental Figure 2a and b). On the other hand, bortezomib had only little effect on PBMCs from healthy donors compared with fresh ATL cells. Furthermore, bortezomib increased phosphorylated IκBα protein, but not nonphosphorylated IκBα protein, in the primary ATL cells (supplemental Figure 2c), which was consistent with the findings observed in Tax nonexpressing cell lines, such as ED(−). These results suggested that bortezomib could induce cell death of not only HTLV-I associated cell lines but also primary ATL cells by blocking the NF-κB pathway.

Discussion

Regardless of the progress in the virological, epidemiological and clinical aspects of HTLV-I and ATL, the prognosis of patients with ATL remains poor. Among the factors implicated in this poor prognosis, immunodeficiency due to impaired cell-mediated immunity and drug-resistance of ATL cells are major obstacles to its treatment.[4] Constitutive NF-κB activation was demonstrated not only in HTLV-I associated cell lines but also in fresh ATL cells regardless of Tax expression,[9] which could contribute to the drug-resistance of ATL cells through over expression of antiapoptotic genes such as *bcl-xL*. In the present study, we have revealed that bortezomib exerted antitumor activity against HTLV-I associated cell lines (*in vitro* and *in vivo*) and fresh ATL cells (*in vitro*). Although several targets have been proposed for the action of bortezomib, including upregulation of p53, p21, and inhibition of NF-κB activation,[11] this study showed the correlation between susceptibility to bortezomib and NF-κB activation, suggesting that NF-κB is the major target of bortezomib in ATL cells.

Recently, caspase-independent cell death has been studied in programmed cell death.[22] When caspases were inhibited by z-VAD-fmk, Fas-mediated signaling could induce necrotic cell death instead of apoptosis.[23,24] Apoptosis was induced in T-lymphocytes treated with NF-κB inhibitor, whereas it could cause nonapoptotic cell death in the presence of z-VAD-fmk.[25] This also suggests that bortezomib-induced cell death is similar to cell death induced by NF-κB inhibition, which strengthen the possibility that inhibition of NF-κB plays a central role in bortezomib-induced cell death.